

AD-A 059 966

AD

MEMORANDUM REPORT ARBRL-MR-02848

(Supersedes IMR No. 403)

INTERNAL PRESSURE FROM EXPLOSIONS IN
SUPPRESSIVE STRUCTURES

Charles Kingery
Robert Schumacher
William Ewing, Jr.

TECHNICAL
LIBRARY

June 1978



US ARMY ARMAMENT RESEARCH AND DEVELOPMENT COMMAND
BALLISTIC RESEARCH LABORATORY
ABERDEEN PROVING GROUND, MARYLAND

Approved for public release; distribution unlimited.

DTIC QUALITY INSPECTED 3

Destroy this report when it is no longer needed.
Do not return it to the originator.

Secondary distribution of this report by originating
or sponsoring activity is prohibited.

Additional copies of this report may be obtained
from the National Technical Information Service,
U.S. Department of Commerce, Springfield, Virginia
22161.

The findings in this report are not to be construed as
an official Department of the Army position, unless
so designated by other authorized documents.

*The use of trade names or manufacturers' names in this report
does not constitute indorsement of any commercial product.*

REPORT DOCUMENTATION PAGE		READ INSTRUCTIONS BEFORE COMPLETING FORM
1. REPORT NUMBER MEMORANDUM REPORT ARBRL-MR-02848	2. GOVT ACCESSION NO.	3. RECIPIENT'S CATALOG NUMBER
4. TITLE (and Subtitle) INTERNAL PRESSURE FROM EXPLOSIONS IN SUPPRESSIVE STRUCTURES		5. TYPE OF REPORT & PERIOD COVERED Final
		6. PERFORMING ORG. REPORT NUMBER
7. AUTHOR(s) Charles Kingery Robert Schumacher William Ewing, Jr.		8. CONTRACT OR GRANT NUMBER(s)
		10. PROGRAM ELEMENT, PROJECT, TASK AREA & WORK UNIT NUMBERS 4932-45-1264001
9. PERFORMING ORGANIZATION NAME AND ADDRESS US Army Ballistic Research Laboratory (ATTN: DRDAR-BLT) Aberdeen Proving Ground, MD 21005		12. REPORT DATE JUNE 1978
		13. NUMBER OF PAGES 80
11. CONTROLLING OFFICE NAME AND ADDRESS US Army Armament Research and Development Command US Army Ballistic Research Laboratory (ATTN: DRDAR-BL) Aberdeen Proving Ground, MD 21005		15. SECURITY CLASS. (of this report) UNCLASSIFIED
		15a. DECLASSIFICATION/DOWNGRADING SCHEDULE
14. MONITORING AGENCY NAME & ADDRESS (if different from Controlling Office)		
16. DISTRIBUTION STATEMENT (of this Report) Approved for public release; distribution unlimited.		
17. DISTRIBUTION STATEMENT (of the abstract entered in Block 20, if different from Report)		
18. SUPPLEMENTARY NOTES This report supersedes BRL Interim Memorandum Report No. 403. The work reported here was performed for, and funded by PA, A 4932 MM&T Project No. 5751264, Advanced Technology for Suppressive Shielding of Hazardous Production and Supply Operations for Production Base Modernization and Expansion Program.		
19. KEY WORDS (Continue on reverse side if necessary and identify by block number) Suppressive Structure Vented Structures Blast Inside Structures Panel Venting Model Tests		
20. ABSTRACT (Continue on reverse side if necessary and identify by block number) (1jc) This report contains a documentation of the blast environment in closed and partially closed cubicles. Tests were conducted using two charge weights (0.5 and 1.0 pound) and eight structures, each with different venting characteristics. Effective vent areas were determined from comparisons of the duration of the quasi-static pressure with those of known vent areas with similar charge to structure volume ratios.		

TABLE OF CONTENTS

	Page
LIST OF ILLUSTRATIONS	5
LIST OF TABLES	7
AUTHORS COMMENTS	9
I. INTRODUCTION	11
A. Background	11
B. Objectives	11
II. TEST PROCEDURE	11
A. Test Structures	12
B. Instrumentation	15
III. RESULTS	19
A. Reflected Pressure Parameters	19
1. Peak Reflected Pressure	20
2. Reflected Pressure versus Time	20
3. Reflected Pressure Duration	27
4. Reflected Pressure Impulse	27
5. Reflected Pressure Impulse versus Time	27
B. Quasi-Static Pressure Parameters	34
1. Peak Quasi-Static Pressure	34
2. Quasi-Static Pressure Duration	38
3. Quasi-Static Pressure Impulse	40
C. Effective Vent Areas	40
1. Effective Vent Area Determined from Quasi-Static Pressure Duration	40
2. Effective Vent Area Determined from Quasi-Static Pressure Impulse	43

TABLE OF CONTENTS (Continued)

	Page
D. Internal Pressure Loading	46
1. Internal Pressure in Structures T-1, T-3, and T-5	46
2. Internal Pressure in Structures 0-1, 0-2, and 0-3	48
3. Internal Pressure in Structure 0-4	51
4. Internal Pressure in Structure N-V	51
5. Internal Pressure in Structure T-5 and 0-4 from 1 Pound Charges	55
6. Internal Pressure in Structure 0-3 from 0.5 and 1.0 Pound Charges	55
E. Internal Pressure versus Time Predictions	55
1. Internal Pressure versus Time for Structures with Different Vent Areas	55
2. Comparison of Measured Records and Computer Output	60
3. A Second Method for Determining the Internal Pressure Decay Rate	60
IV. CONCLUSIONS	66
LIST OF SYMBOLS	68
REFERENCES	69
DISTRIBUTION LIST	71

LIST OF ILLUSTRATIONS

Figure	Page
1a. Test Fixture Assembly for "T" Type Structures	13
1b. Test Fixture Assembly for "O" Type Structures	14
2. Gage positions	17
3. BRL Shock Isolation Transducer Mount	18
4. Peak Reflected Pressure versus Scaled Distances	22
5. Reflected Pressure versus Time - P7 (T-5 and 0-2)	23
6. Reflected Pressure versus Time - P7 (0-4 and NV)	24
7. Reflected Pressure versus Time - P8 (T-5 and 0-2)	25
8. Reflected Pressure versus Time - P8 (0-4 and NV)	26
9. Scaled Reflected Pressure Duration versus Scaled Distance	28
10. Scaled Reflected Pressure Impulse versus Scaled Distance	29
11. Reflected Impulse versus Time - P7 and P8 for T-5	30
12. Reflected Impulse versus Time - P7 and P8 for 0-2	31
13. Reflected Impulse versus Time - P7 and P8 for 0-4	32
14. Reflected Impulse versus Time - P7 and P8 for NV	33
15. Method of Determining P_{QE} and P_{QA}	36
16. P_{QE} versus Charge Weight to Structure Volume Ratio	37
17. P_{QA} versus Charge Weight to Structure Volume Ratio	39
18. Scaled Venting $(V/A)/w^{1/3}$ versus Scaled Duration $tg/w^{1/3}$	44
19. Internal Pressure versus Time at P9 in Structures T-1, T-3, and T-5, 0.5 Pound Charge	47

LIST OF ILLUSTRATIONS (Continued)

Figure		Page
20.	Compressed Time Scale Showing Complete Pressure Pulse For T-5	49
21.	Internal Pressure versus Time at P9 in Structure 0-1, 0-2, and 0-3, 0.5 Pound Charge	50
22.	Compressed Time Scale Showing Complete Pressure Duration of Figure 21 Records	52
23.	Comparison of Internal Pressure versus Time Recorded in Structure 0-4 and Structure T-5	53
24.	Comparison of Internal Pressure versus Time Recorded in Structure N-V and Structure 0-3	54
25.	Comparison of Internal Pressure versus Time Recorded in Structure T-5 and 0-4 from a 1.0 Pound Charge	56
26.	Comparison of Internal Pressure versus Time Recorded in Structure 0-3 from 0.5 and 1.0 Pound Charges	57
27.	Computed Internal Pressure versus Time for Different Vent Areas	58
28.	Computed Time versus Vent Area for Constant Internal Pressure, 0.5 Pound Charge	59
29.	Computed Time versus Vent Area for Constant Pressure, 1.0 Pound Charge	61
30.	Comparison of Measured Data from T-1 and the Computer Output for a 9.3 Percent Vent Area	62
31.	Comparison of Measured Data from T-5 and Computer Output for a 4.7 Percent Vent Area	63
32.	Comparison of Measured Data from Structure 0-4 and Computer Output for a 4.7 Percent Vent Area	64
33.	Comparison of Measured Data from Structure 0-3 and Computer Output for 2.4 Percent Vent Area for Two Charge Weights	65
34.	Comparison of Two Prediction Methods of Internal Pressure versus Time with Measured Data	67

LIST OF TABLES

Table	Page
I. Identification of Test Configurations	16
II. Average Reflected Pressure Parameters P7 and P8	21
III. Average Quasi-Static Pressure Parameters P9	35
IV. Effective Vent Area - Function of Duration t_g	41
V. Effective Vent Area - Function of Impulse I_g	45

AUTHORS COMMENTS

The English system of units are utilized exclusively in this report. This was done in order that the results of this experimental program would be compatible with the previous efforts and reports pertaining to the Category I shield development. In particular, the results are intended for use in structural design evaluations, evaluating compatibility with specifications in the DOD Explosive Safety Standards and to be compatible with predictions, analyses and design effort of other category shield programs which utilize the English system of units.

The use of double scales and/or conversion factors throughout this report was considered but not included because of the considerable effort and expense involved for what would be of minor benefit to the principal users of this report.

I. INTRODUCTION

A. Background

This work is part of the Category Shield Program and is specifically related to Category I. The Category I Shield is being designed to contain the fragments and attenuate the airblast from an accidental explosion in a melt-pour operation containing 2500 pounds of explosive. The size of the structure was to be a 40 foot cube.* The peak overpressure must be attenuated to 50 percent of that expected at a scaled intraline distance of 18 (ft/lbs^{1/3}) without shielding.

In order to construct a cost-effective Category I Shield, the necessary critical design information was not available. Both BRL and a contractor, Southwest Research Institute (SwRI) recommended that a 1/4 scale structure be designed and tested with required instrumentation. This recommendation was accepted by Edgewood Arsenal. Because of the large number of candidate panel designs, and the lack of knowledge of the effect of their venting characteristics on the decay of the internal gas pressure and blast attenuation outside, BRL investigators suggested that a 1/16 size structure be made for each candidate panel and that tests be conducted with scaled charge weights.

Eight 1/16 size structures were constructed at the National Space and Technology Laboratory (NSTL), Bay St. Louis, Mississippi and shipped to BRL for testing.

B. Objectives

The objectives of this phase of the Category I Shield program are:

1. To document and present in a usable format the blast loading versus time generated at the walls of eight 1/16 - size structures from an internal explosion.

2. To determine the effective vent area ratios of selected candidate panels based on a comparison of the measured decay rate of the internal gas pressure with that of several prediction methods.

II. TEST PROCEDURE

Test procedures followed in designing the experiment are described below. The gages were selected based on the anticipated environment, then calibrated and integrated with the proper mounts, amplifiers, and recording system.

**The design was later changed to a cylindrical structure with the same volume.*

Spherical 50/50 pentolite charges having nominal weights of 0.5 and 1.0 pounds were fired in the geometric center of each structure to bracket the scaled charge weights of 0.61 pounds ($2500 \times 1/16^3$) and a 25 percent overweight of 0.76 pounds.

A. Test Structures

The test structures are not true scaled models because the components; i.e., I-beams, angle irons and perforated plates are the same size as planned for the 1/4 scale structure. Scaling by 1/16 reduces the interior dimension to 2.50 feet (as-built 2.58 feet) and the volume by $1/16^3$. Figure 1a and 1b are drawings showing the details of the type "T" and type "O" structures. There were three type "T" structures, four type "O" structures and one closed or non-venting structure. The sub-scale structural description was based upon the fabrication drawings prepared by the General Electric Co. at the NSTL, Bay Saint Louis, Mississippi (DWG 1E700F33012). Figure 1 includes only those details that are considered important for documenting the physically significant characteristics. The three interlocking I-beam cubicles were given the notation of T-1, T-3, and T-5 which corresponds to the identification of structures Type 1, 3, and 5 in Figure 1a. The configurations utilizing perforated plates in this design were given the notation O-1 through O-4, these correspond to the cubicles identified as options 1 through 4 in Figure 1b.

A method for calculating the effective vent area A_{eff} was developed by SwRi¹ based on airblast attenuation outside of the structure. The spacing of the panel components and the vent area of the individual perforated plates were designed using this method. It is described as follows:

1. The vent area for each element of each panel was determined.

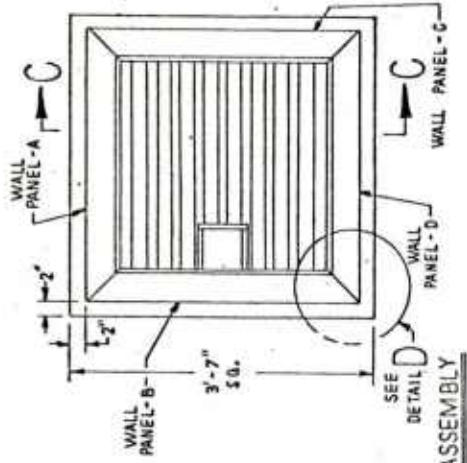
a. For angle iron configurations - the distance between flanges of adjacent angles was determined. This distance was multiplied by the total number of spaces between members and this result multiplied by the length of the gap between angles (30 inches) to give vent area, A_v .

b. For I-Beam configurations - the distances between flanges and/or between flange and adjacent web were summed for each of the 4 planes in which the I-beam flanges were located. These distances were then multiplied by the length of the gap between I-beams (30 inches) to give vent area, A_v , for each plane.

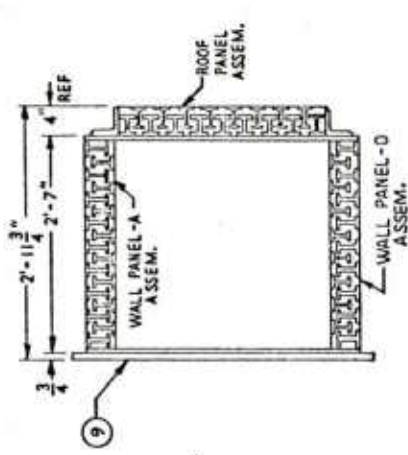
c. For plate configurations - the cross-sectional area per drilled hole per plate was determined and multiplied by the number of holes per plate to give vent area, A_v , for each plate.

¹Baker, W. E., Westine, P. S., et al, "Analysis and Preliminary Design of a Suppressive Structure for a Melt Loading Operation," Tech. Report No. 1, Southwest Research Institute, San Antonio, Texas, March 1974.

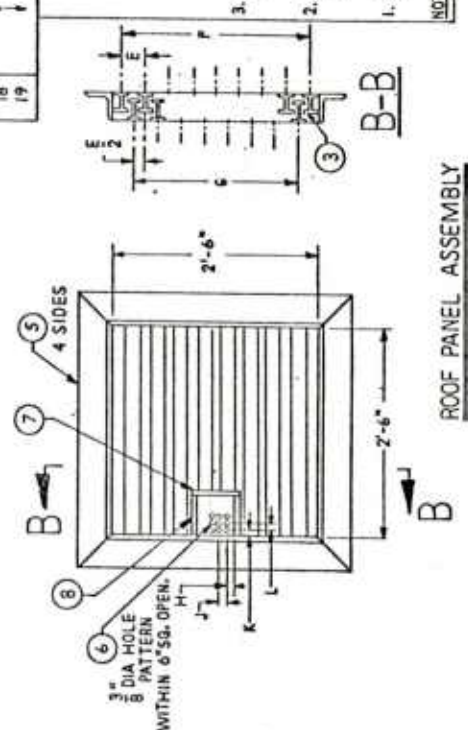
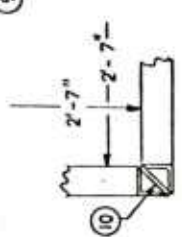
PART	MATERIAL
1	4X4 X 1/2" L X 2'-6" LG.
2	1/2" X 4" X 3'-2 1/2" LG. MILD STL.
3	3" X 5.7 I X 2'-6" LG.
4	1" SCH. 40 STL PIPE X 5' LG. ϕ
5	4" X 1/2" L X 3'-2" LG.
6	1/2" X 7" X 7" MILD STL. PL.
7	1/2" X 4" X 7" STL. PL.
8	1/2" X 4" X 6" STL. PL.
9	3/4" X 3'-7" SQ. STEEL PL.
10	1/2" X 5" X 2'-7" LG.
11	10 GA. PL. X 2'-6" SQ. PERF. WITH 1/8" ϕ HOLES ON .65% .699 CENT.
12	1" X 1" X 1/8" X 2'-6" STR. STL.
13	3/16" PL. X 2'-6" SQ. PERF. WITH 3/16" ϕ HOLES ON 1" F. 69 CENT.
14	1 1/4" X 1 1/4" X 3/16" X 2'-6" LG.
15	3/16" PL. X 2'-6" SQ. PERF. WITH 3/16" HOLES ON 1" F. 531 CENT.
16	3/16" PL. X 2'-6" SQ. PERF. WITH 3/16" ϕ HOLES ON 1/2" CENT. SQ.
17	1" SCH. 40 STL PIPE X 3' X 3' 1/4" LG.
18	X 4' X 1 1/4" LG.
19	X 3' LG.



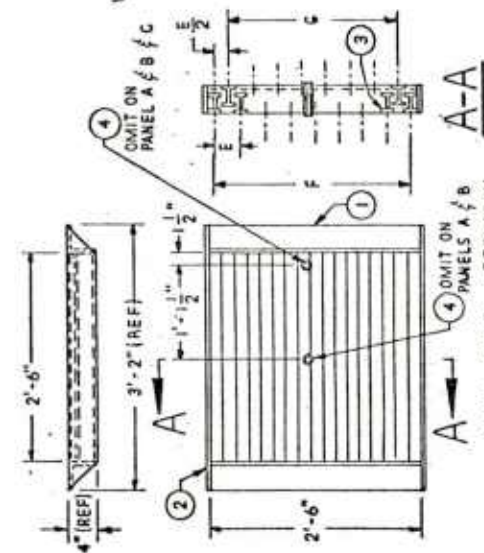
TEST FIXTURE FINAL ASSEMBLY



TYP WALL CORNER
DETAIL D



ROOF PANEL ASSEMBLY



WALL PANEL ASSEMBLY

1. PARTS 4, 17, 18 & 19 ARE THREADED THRU 1 1/8" - 12 NF.
2. ALL ASSEMBLIES ARE OF CONTINUOUS FILLET WELD CONSTRUCTION.
3. THIS DWG. NOT COMPLETE WITHOUT SHEET 2.

NOTES:

CAT. I
TEST FIXTURE ASSEMBLY

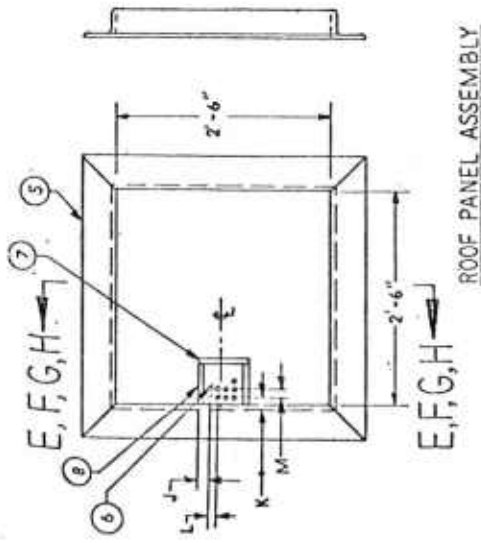
I BEAM STRUCTURE
(TYPE 1, 3 & 5)

SHEET 1 OF 2

TYPE	H	J	K	L	HOLES	REQ'D.
1	.312	.500	.343	.530	132	1
3	.412	.599	.412	.599	81	1
5	.608	.795	.608	.795	49	1

TYPE	E	F	G	EQ. SPA	EQ. SPA	REQ'D.
1	3.459	1.729	8	7	4	4
3	3.07	1.53	9	8	4	4
5	2.76	1.38	10	9	4	4

Figure 1a. Test Fixture Assembly for "I" Type Structures



HOLES IN DOOR DIMENSIONS					
	J	K	L	M	HOLES
OPTION 1	2"	2"	1 1/2"	1"	12
OPTION 2	1 1/2"	1 3/4"	1"	1 3/4"	20
OPTION 3	1 1/2"	1 1/2"	1"	1"	25
OPTION 4	1 1/4"	1 1/4"	3/4"	3/4"	49

4. * PART 11 — 1890 HOLES/PLATE
 PART 13 — 1218
 PART 15 — 1595
 PART 16 — 3249

ALL PERF. PLATE MUST BE CUT AND
 ALIGNED SO THAT HOLES DO NOT
 LINE UP (LINE OF SIGHT)

3. THIS DRAWING NOT COMPLETE
 WITHOUT SHEET 1.

2. SEE SHEET 1 FOR MATERIAL &
 NEXT ASSEMBLY.

1. DIMEN. NOT SHOWN ARE SAME AS PANEL
 DIMEN. ON SHEET 1.

NOTES :

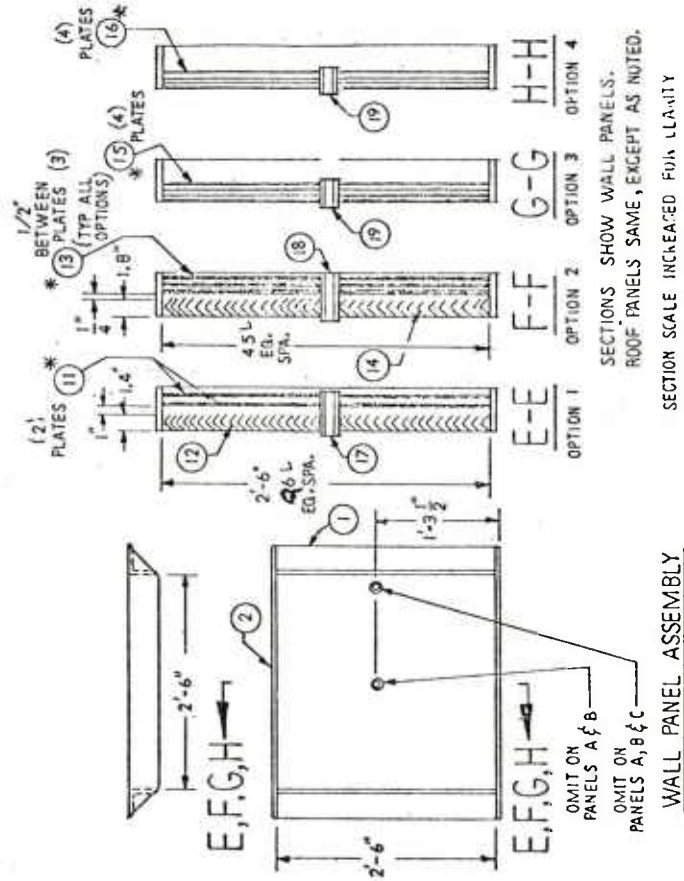


Figure 1b. Test Fixture Assembly for "O" Type Structures

2. The vent area for each element of each panel was used to determine the effective vent area for each panel using the following relationship.

$$\frac{1}{A_v} = \frac{1}{A_1} + \frac{1}{A_2} + \dots + \frac{1}{A_n} \quad (1)$$

n = number of venting elements.

For the "T" configurations four vent areas (A_i) would be combined, for the 0-1 configuration three vent areas would be combined, and for configurations 0-2 through 0-4 four vent areas would be combined.

3. The effective vent area ratio, for a given configuration, was determined by multiplying the effective vent area per panel by the number of vented panels per structure (5 for our cubicles) and dividing the result by the internal surface area of the 5 panels.

The effective vent area ratios determined by BRL using the preceding method are listed in Table I for all test structures.

B. Instrumentation









The primary objective of this report is to present a record of the gas and shock pressure generated within a structure when high explosive charges are detonated in the geometric center of the structure. Two of the measurements (P7 and P8) record peak reflected pressure data, and one (P9) measured quasi-static pressure data. The location of all gages are shown in Figure 2. A special gage mount (Figure 3) isolated the pressure transducers from the severe mechanical shock and vibration environment of the panels they were attached to. Gage location P8 did not utilize the protective shield (bottom plates) as indicated in Figure 3 so that the gage mount would have a minimal effect on the ability to indicate the high reflected overpressure shocks that were to be measured.

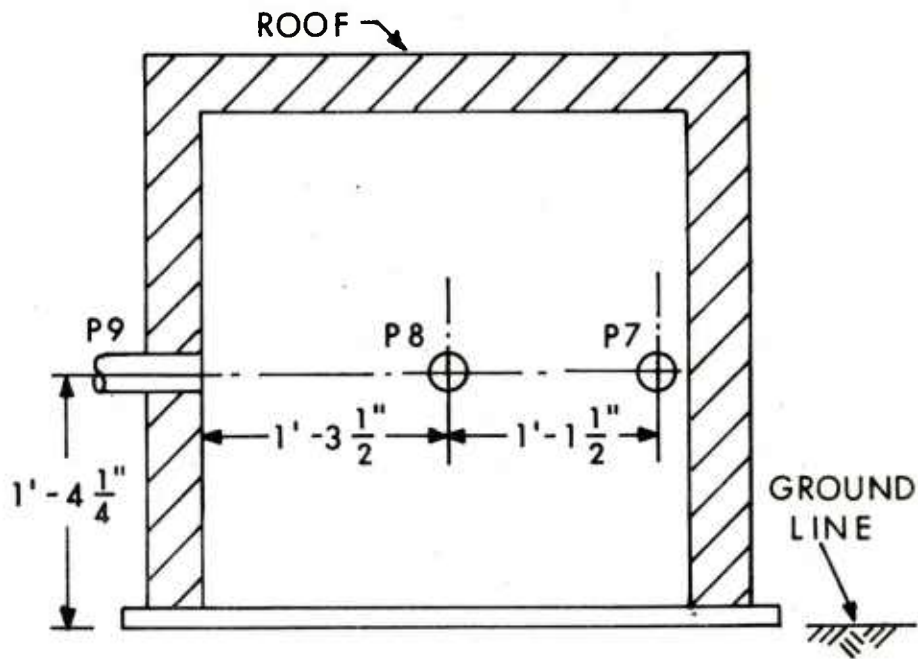
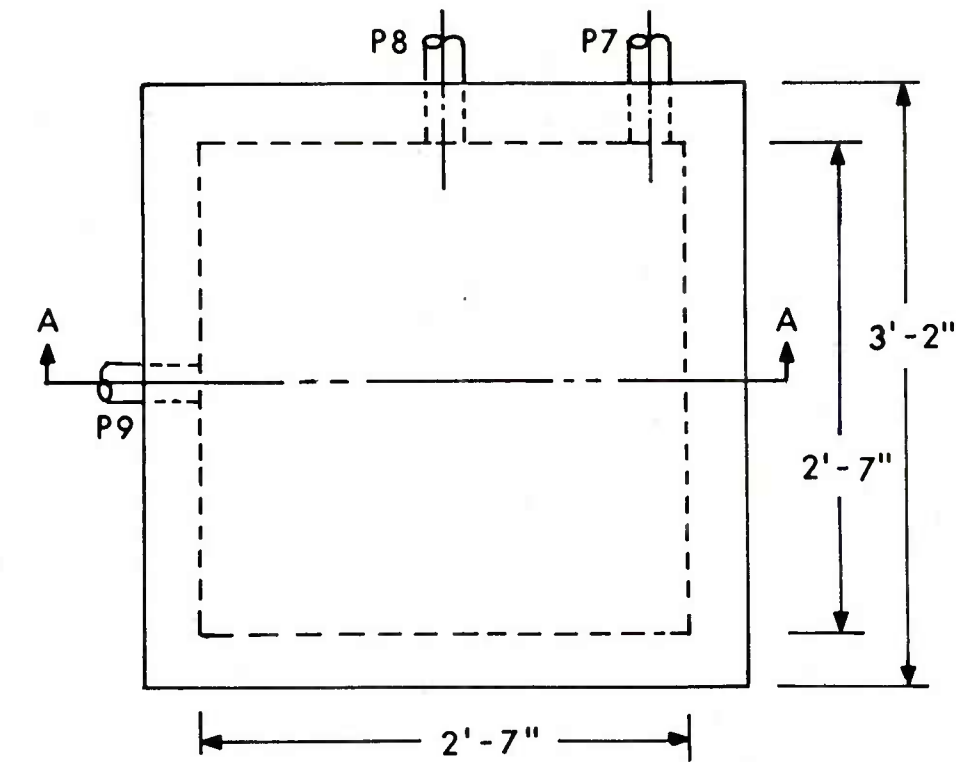
Gages P7 and P8 were tuned to measure the high frequency shock pressure fluctuations and therefore were not expected to be too effective in indicating the quasi-static pressure fluctuations which were at much lower pressures. Gage P9 was included to measure the quasi-static pressure fluctuations inside the enclosure. Therefore, its upper frequency response and full scale pressure recording level were reduced so that the high frequency and high pressure shocks would have a minimal detrimental effect on the desired measurements.

Locations P7 and P8 utilized Susquehanna Instrument Model ST-4 gages having a tourmaline sensing element. These gages have a natural frequency of 1.5 m Hz, and installed time constant of 4 seconds, and a useful indication capability over the pressure range between 10 and 10,000 psi. These gages were of the piezo-electric type and utilized in-line source followers.

NOTE: A_{eff} and A_v are used interchangeably to denote effective vent area.

Table 1. Identification of Test Configurations

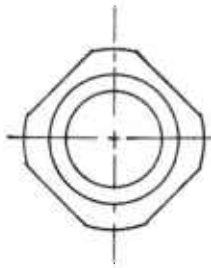
NOTATION	BOX CONSTRUCTION	WALL CONFIGURATION	EFFECTIVE VENT AREA	
			FT ²	RATIO
T-0	N/A (FREE FIELD REF.)	N/A	N/A	1.0000
T-1	INTERLOCKING BEAMS		2.166	0.0649
T-3	INTERLOCKING BEAMS		1.493	0.0448
T-5	INTERLOCKING BEAMS		0.777	0.0233
O-1	ANGLE IRON +2 PERFORATED PLATES		0.386	0.0116
O-2	ANGLE IRON +3 PERFORATED PLATES		0.378	0.0113
O-3	4 PERFORATED PLATES		0.382	0.0115
O-4	4 PERFORATED PLATES		0.777	0.0233
N-V	NON-VENTED SOLID PLATES		≈0	≈0



SECTION A - A

Figure 2. Gage Positions

TOP PLATE
MTL - STAINLESS STEEL



$\frac{7}{8}$ " SQUARE TO
FOR WRENCH

INSERT
MTL - NYLON OR TEFLON

NO. 2-16
PARKER O-RINGS
MAKE ALL GROOVES
.035 - .037 DEEP
.075 - .080 WIDE

CASE
MTL - STAINLESS STEEL

BOTTOM PLATES
MTL - STAINLESS STEEL

4 - SCREWS
2-56 NC $\frac{3}{8}$ " LONG

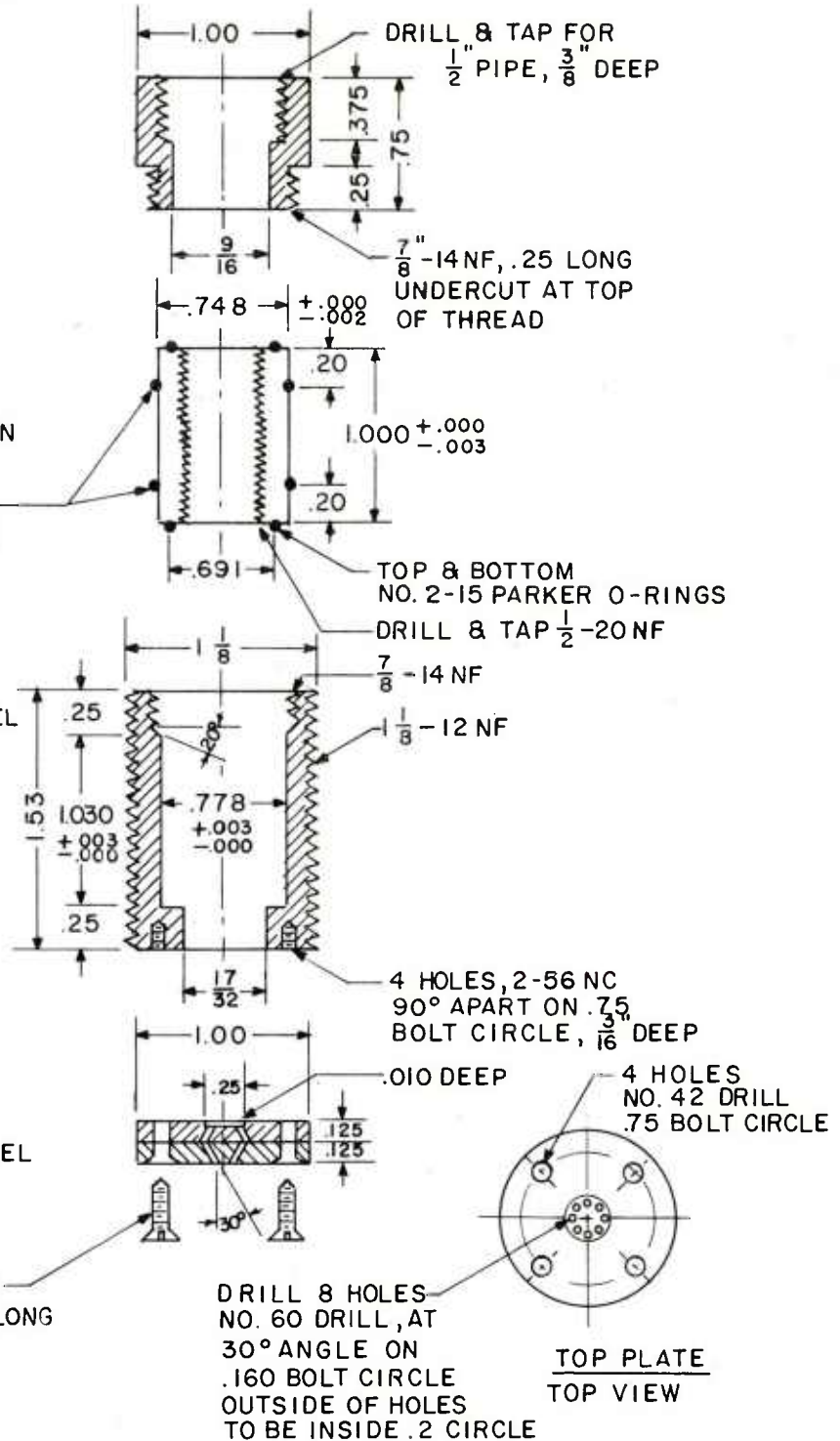


Figure 3. BRL Shock Isolation Transducer Mount

Location P9 utilized a Quartz sensing element piezo-electric type pressure transducer with attached source follower. The gage was a PCB Electronics Inc. Model 113A22. This gage has a natural frequency of 500 k Hz, an installed time constant of 2 seconds, and a useful pressure indication capability over the pressure range between vacuum and 6000 psi.

The signals from the pressure transducers were amplified as necessary by using Newport Laboratory Inc. Model 60-S D.C. amplifiers having an adjustable upper frequency cut-off which was set at 100 k Hz for measurements at P7 and P8 and at 10 k Hz for measurements at P9. This was permissible because the measurement at P9 was intended to indicate only the quasi-static pressure variation produced inside the test structure. In addition, the lowered high-frequency cut-off would minimize overdriving the recording system as a result of the very high shock pressure that would be sensed prior to the quasi-static pressure of interest.

All pressure data were recorded on a Honeywell Model 7600 tape recorder having a frequency response from D.C. to 80 k Hz. This established the upper frequency limit for all measurements except P9 which was previously limited to 10 k Hz. The low frequency capability of the system was limited by the characteristics of the pressure transducers as determined from the time constants indicated above.

For several tests, toward the end of the program (configurations 0-3, 0-4, and N-V) measurements at P8 were recorded on an oscilloscope as well as on the tape recorder, in an attempt to determine the amount of peak overpressure loss that could be expected from the tape recorded data. The upper frequency for this measurement was still limited to 100 k Hz by the instrumentation amplifier in the circuit between the transducer and the oscilloscope.

III. RESULTS

A total of 58 test firings was conducted. All charges were located in the geometric center of the structure. The blast parameters recorded at the three gage locations are presented in the following sections in the form of tables and curves. Reflected pressure parameters are compared with accepted standard references and effective vent areas are calculated from the quasi-static pressure durations.

A. Reflected Pressure Parameters

The reflected pressure impinging on the interior surfaces of the structure were measured at two locations. The locations P7 and P8 are shown in Figure 2. Special gages and mounts were used to record the high pressure and short duration associated with the reflected pressure pulse. Documenting the reflected pressure shock parameters for comparison with theoretical values or other experimental work is difficult because of the changes in the roughness of the reflecting surface, the thermal

environment, detonation products, gas pressure, the short time duration and the repeated reflecting shocks. The data obtained are presented in tables and graphs in the following sections.

1. Peak Reflected Pressure. The peak reflected pressure is defined here as the peak value of the first shock arrival and is not necessarily the maximum reflected pressure. The average value of the peak reflected pressure recorded at P7 and P8 for the two charge weights detonated in the type "T", "O", and un-vented structures are listed in Table II. The average values listed in Table II are plotted versus scaled distance in Figure 4. Also plotted in Figure 4 as a solid line are the reflected pressures versus scaled distance taken from Reference 2. It is clearly evident that measured values fall far below the theoretical curve. This is caused by the limit in the frequency response of the recorder. Based on work reported in Reference 3 a loss of 20 percent of the peak reflected pressure could be expected in the 1000 psi range and a loss of 40 percent in the 5000 psi range. Accounting for these losses would bring the measured values closer to predicted theoretical values. Because of the higher frequency response the oscilloscope data for P8 are closer to the predicted curve than the tape recorded data. The large scatter of the data is due to the differences in structure reflecting surfaces.

2. Reflected Pressure versus Time. Computer plots of the reflected pressure versus time recorded at gage positions P7 and P8 from a 1 pound charge are presented in Figures 5, 6, 7, and 8 for four of the eight structures.

In Figure 5 the recordings at gage position P7 in structure T-5 (I-beam) and structure O-2 (iron) are presented for the first 10 msec. The first shock reflection is the one moving across the wall of the structure while the second reflection, which is of greater magnitude, is produced by the interaction of the adjacent side wall reflection moving out of the corner and passing back over the gage. Also shown in Figure 5 are multiple reflections from the corners and center of the structure. The difference in pressure decay is a function of the effective venting.

In Figure 6 records from P7 are again presented from structure O-4 (perforated plates) and structure N-V (non venting). Here the same phenomena are recorded. The primary difference is the magnitude of the peak reflected pressures. Only the first 0.6 msec of record is considered valid for reflected pressure studies.

²Kingery, C. and Pannill, B., "Parametric Analysis of the Regular Reflection of Air Blast," BRL Report 1249, June 1964.

³Minutes of the Fifteenth Explosives Safety Seminar, Giglio Tos, L., Linnenbrink, T., "Airblast Pressure Measurement Systems and Techniques," Pages 1359 - 1402, September 1973.

Table II. Average Reflected Pressure Parameters
for Measurements P7 and P8

Configu- ration	Nominal Charge Weight (lb)	Peak Pressure (psi)		Time Duration (ms)	Impulse (psi-ms)
		P7	P8*		
T-1	0.5	1035	2440	.22	71
	1.0	1322	3720	.27	125
T-3	0.5	980	2190	.23	74
	1.0	1655	4200	.28	122
T-5	0.5	300	1270	.37	74
	1.0	490	2580	.50	121
O-1	0.5	527	2580	.23	79
	1.0	610	2990	.30	119
O-2	0.5	460	1940	.27	97
	1.0	660	3590 (3990)	.22	138
O-3	0.5	682	2240	.21	99
	1.0	1015	3080 (3760)	.24 (.24)	114 (108)
O-4	0.5	597	2120 (3145)	.23 (.23)	73 (68)
	1.0	654	3375 (4040)	.23 (.23)	122 (111)
N-V	0.5	452	1590 (2100)	.20 (.20)	71 (66)
	1.0	708	3510 (3940)	.20 (.20)	127 (131)

* Numbers in parenthesis are values determined from oscilloscope records having a higher frequency response capability than the magnetic tape recorder. (see section 2 part B)

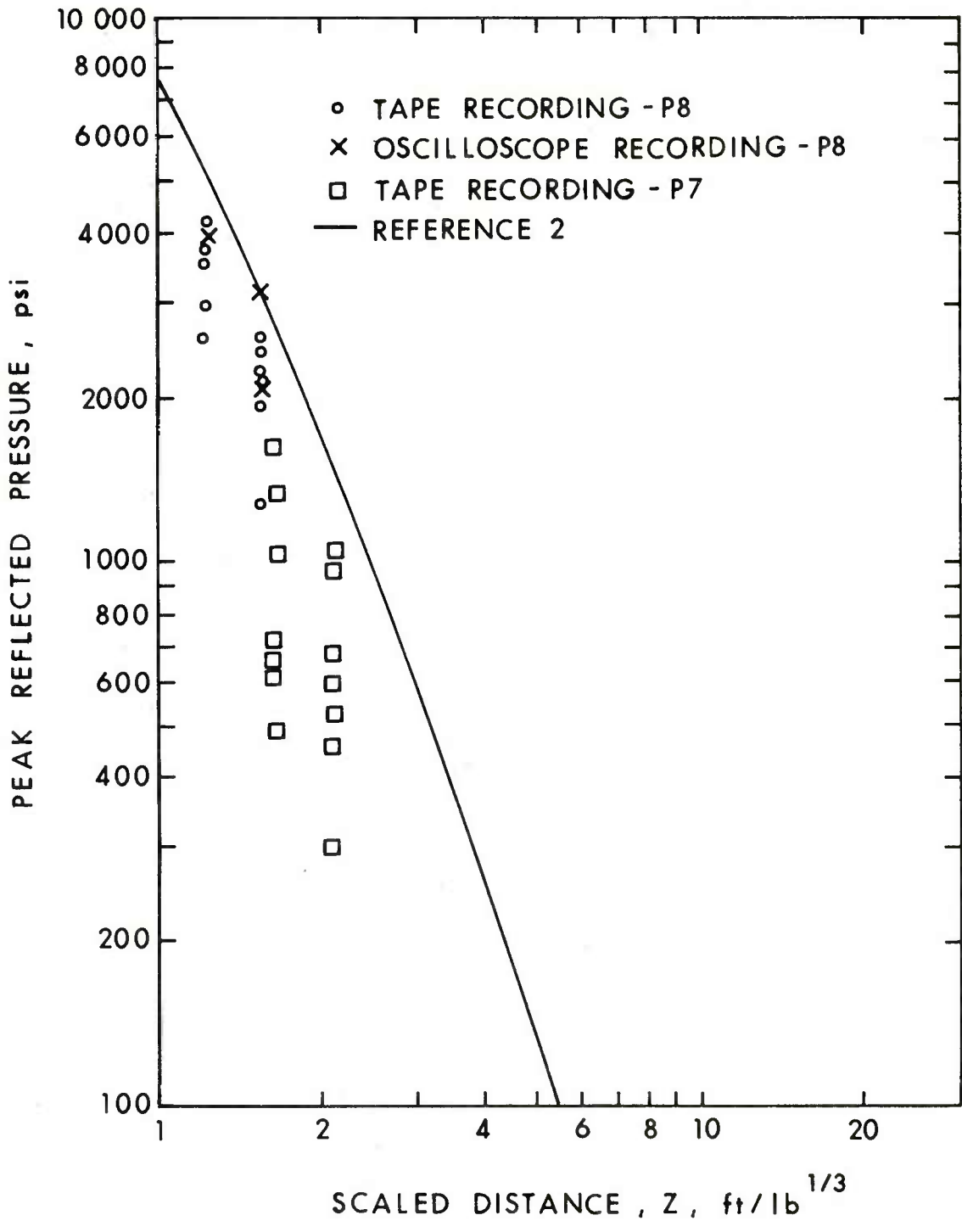


Figure 4. Peak Reflected Pressure versus Scaled Distances

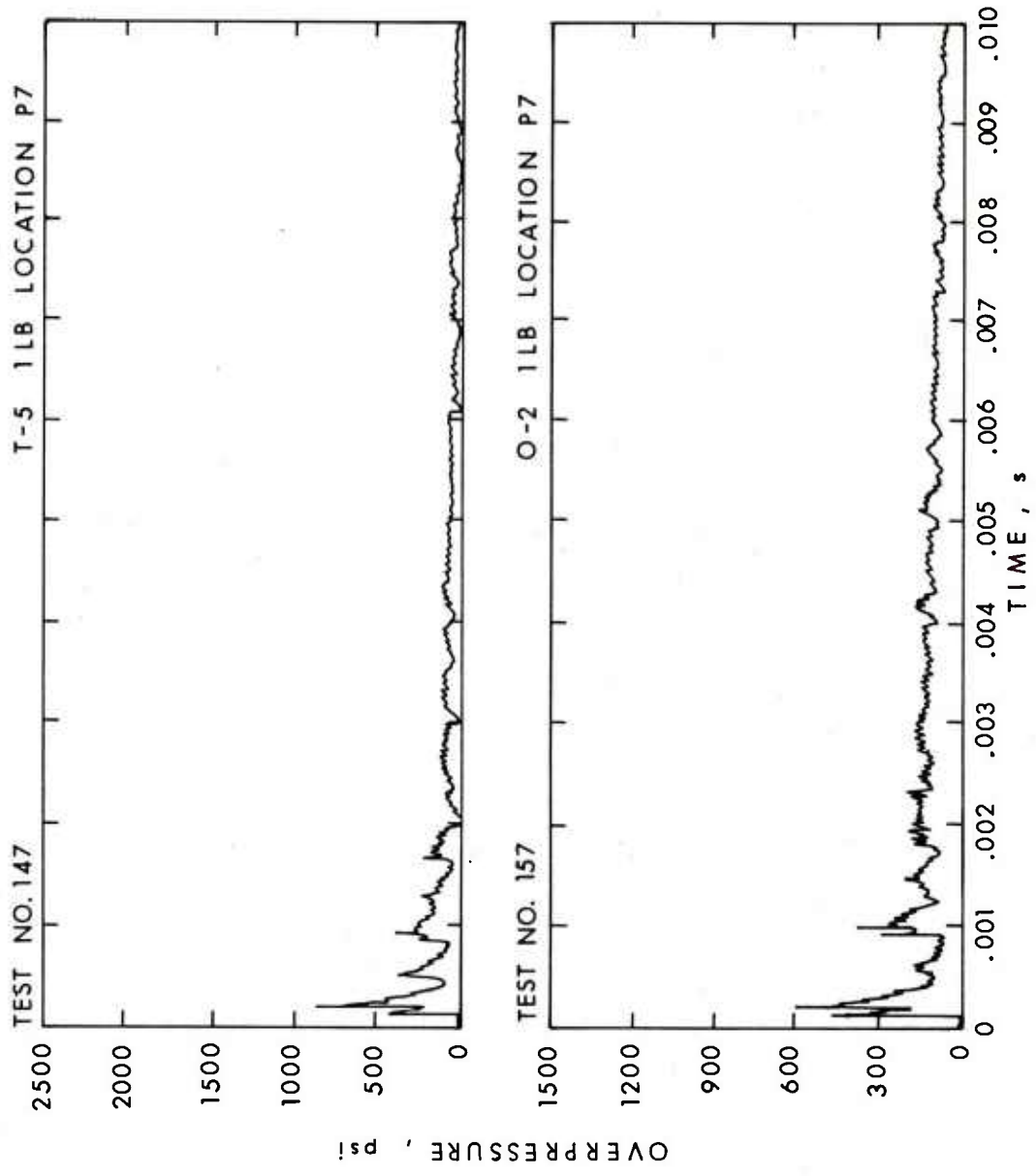


Figure 5. Reflected Pressure versus Time - P7 (T-5 and O-2)

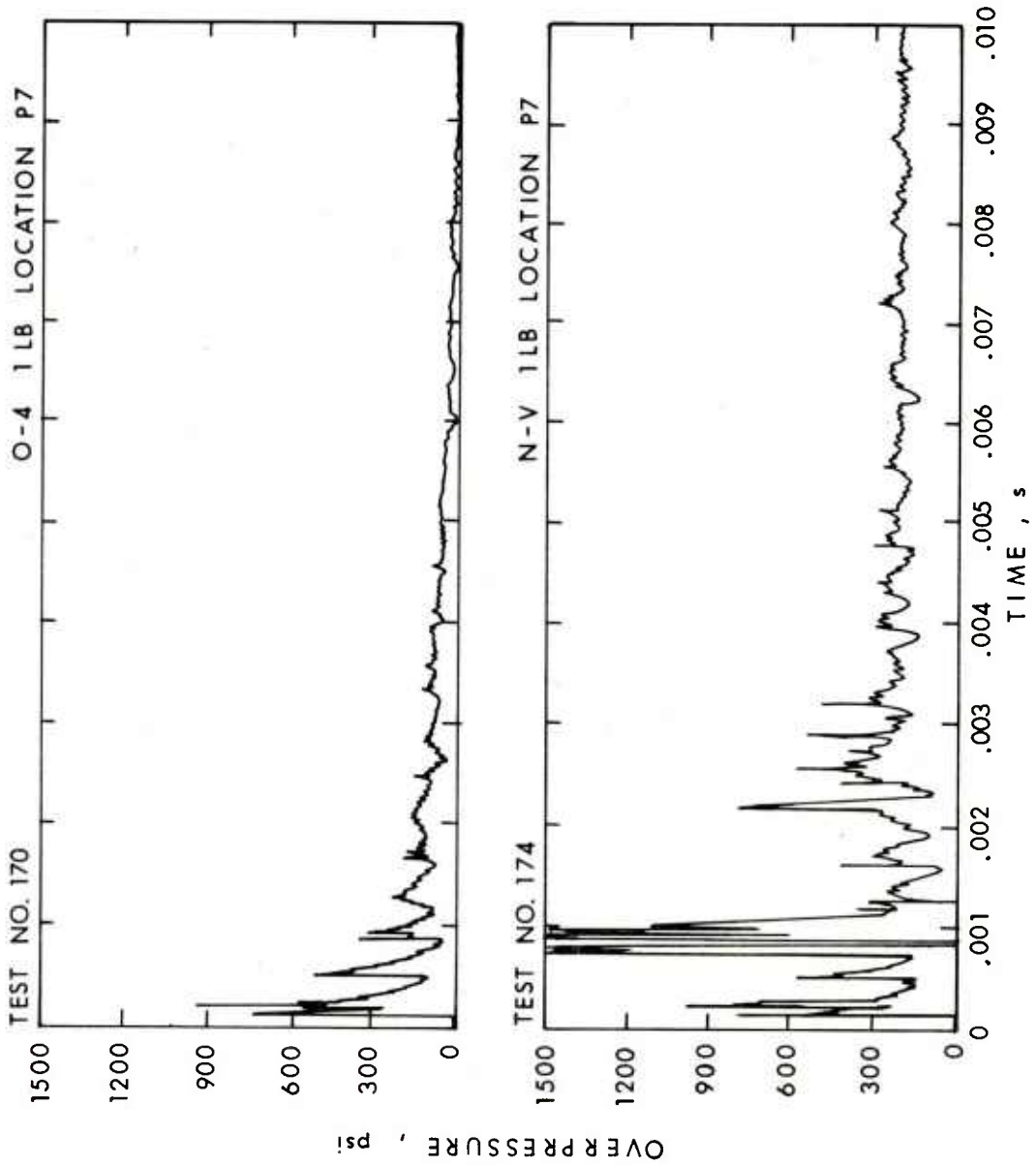


Figure 6. Reflected Pressure versus Time - P7 (O-4 and NV)

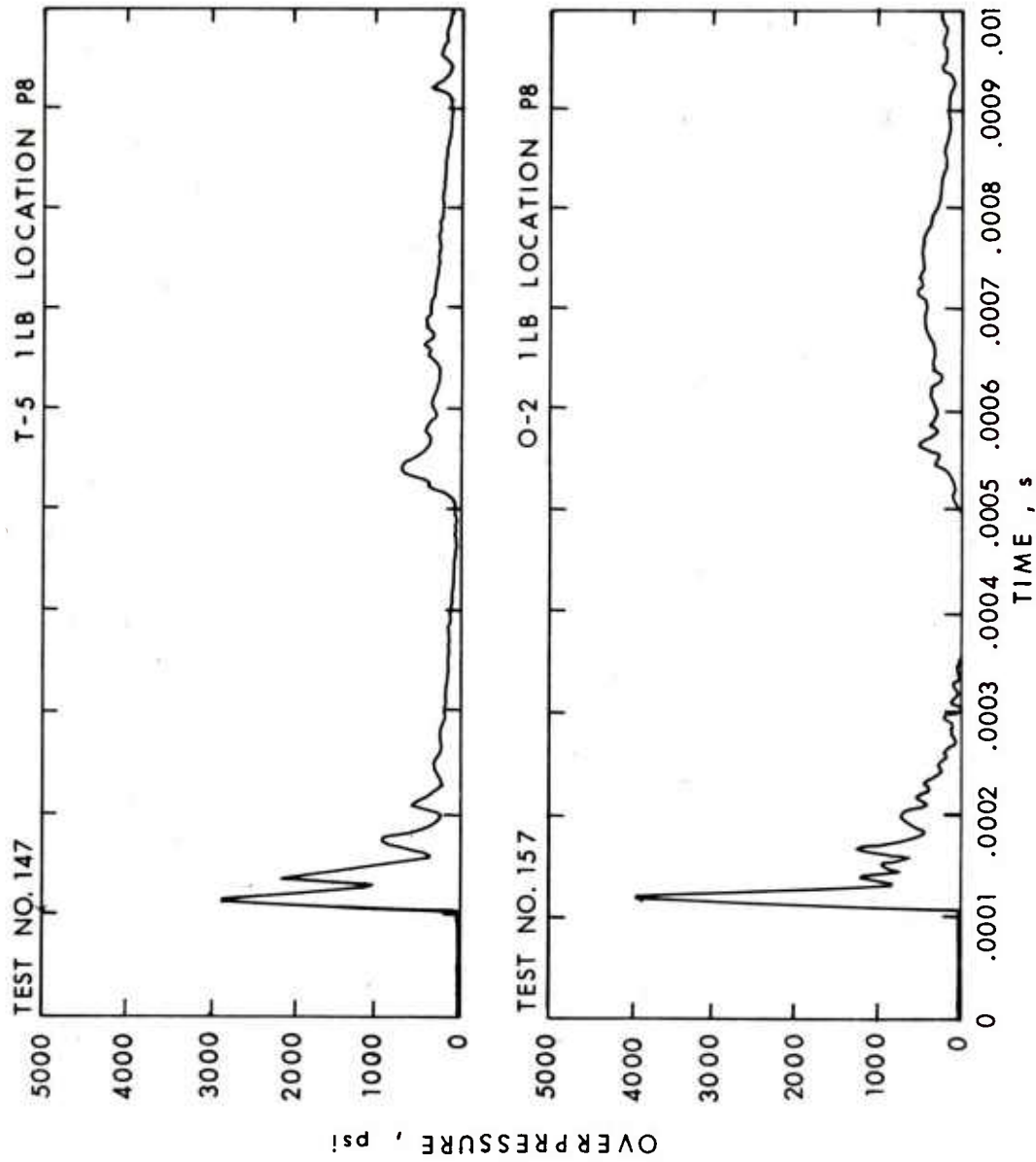


Figure 7. Reflected Pressure versus Time - P8 (T-5 and O-2)

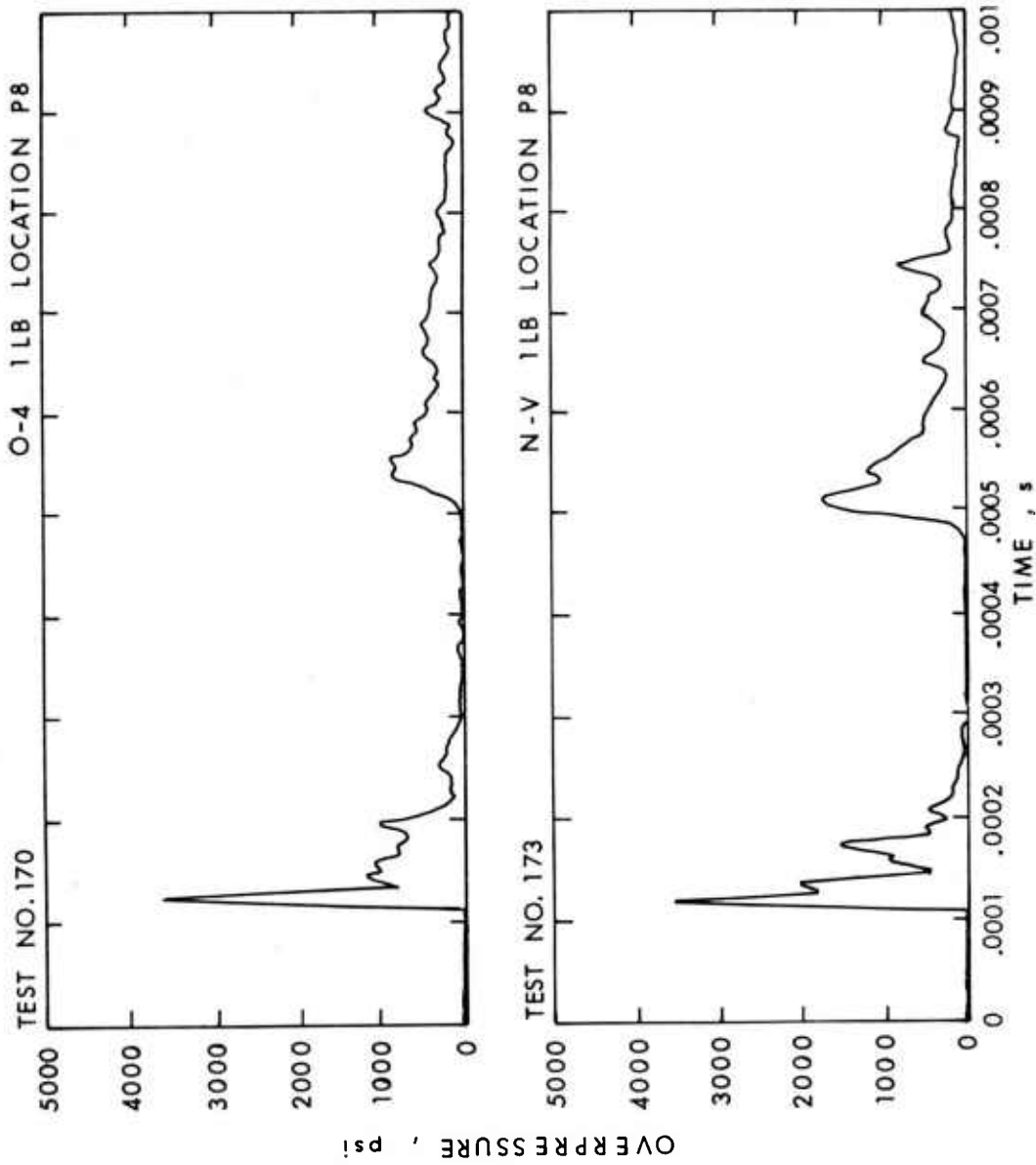


Figure 8. Reflected Pressure versus Time - P8 (O-4 and NV)

Gage position (P8 is in the center of a side wall and should record the normal reflection of the first shock arrival. In Figure 7 the reflected pressure versus time tape recorded at (P8) for a 1 pound charge fired in structures T-5 and 0-2 is presented for a time period of one millisecond. Although the initial reflected pressures recorded in structure T-5 is lower than that recorded in structure 0-2, it should be noted that the second reflections are quite different. The pressure in the 0-2 structure has a slower rise and is much lower than that recorded in structure T-5. This lowering of the second reflected pressure is apparently a function of surface roughness. It can be seen in Table I that the interior surface of structure 0-2 was quite rough.

In Figure 8 the two pressure versus time plots are presented from (P8) as tape recorded in structures 0-4 and N-V. Here again the peak reflected pressures are quite similar but the second reflected pressure is higher in the non-vented structure because of the smooth wall surface.

3. Reflected Pressure Duration. The duration of the reflected pressure is another blast parameter used in describing the loading on the wall of a structure. The durations recorded at P8 were measured for all structures and average values are listed in Table II. The values of scaled duration versus scaled distances are plotted in Figure 9. The values have less meaning for blast loading on the interior walls of a structure than reflected pressure on a plane wall in free field blast because of the repeated reflections, plus the build-up of internal gas pressure. The solid line in Figure 9 was taken from Reference 4. The data from this series of tests are found to vary about the reference curve, with the exception of configuration T-5, where the duration was found to be considerable longer than expected.

4. Reflected Pressure Impulse. The impulse in the first reflected shock is listed in Table II for gage location P8. The scaled impulse versus scaled distance for the two charge weights are plotted in Figure 10. The solid curve plotted in Figure 10 was taken from experimental results reported in Reference 4. The reflected pressure impulse values recorded on this series of tests are approximately 20% lower than those reported in Reference 4, but it should be noted that the surface was not "ideal and the frequency response of the recorders was not optimum.

5. Reflected Pressure - Impulse versus Time. The reflected pressure impulse is one of the primary blast loading parameters. Therefore, the reflected pressure impulse versus time for a maximum of 500 psi-msec of the record obtained from gages P7 and P8 from a 1 pound charge are presented in Figures 11, 12, 13, and 14 for four of the eight structures. These figures indicate the difference in impulse as a function of time

⁴Jack, W. H. "Measurements of Normally Reflected Shock Waves from Explosive Charges," BRL Memo Report No. 1499, July 1963.

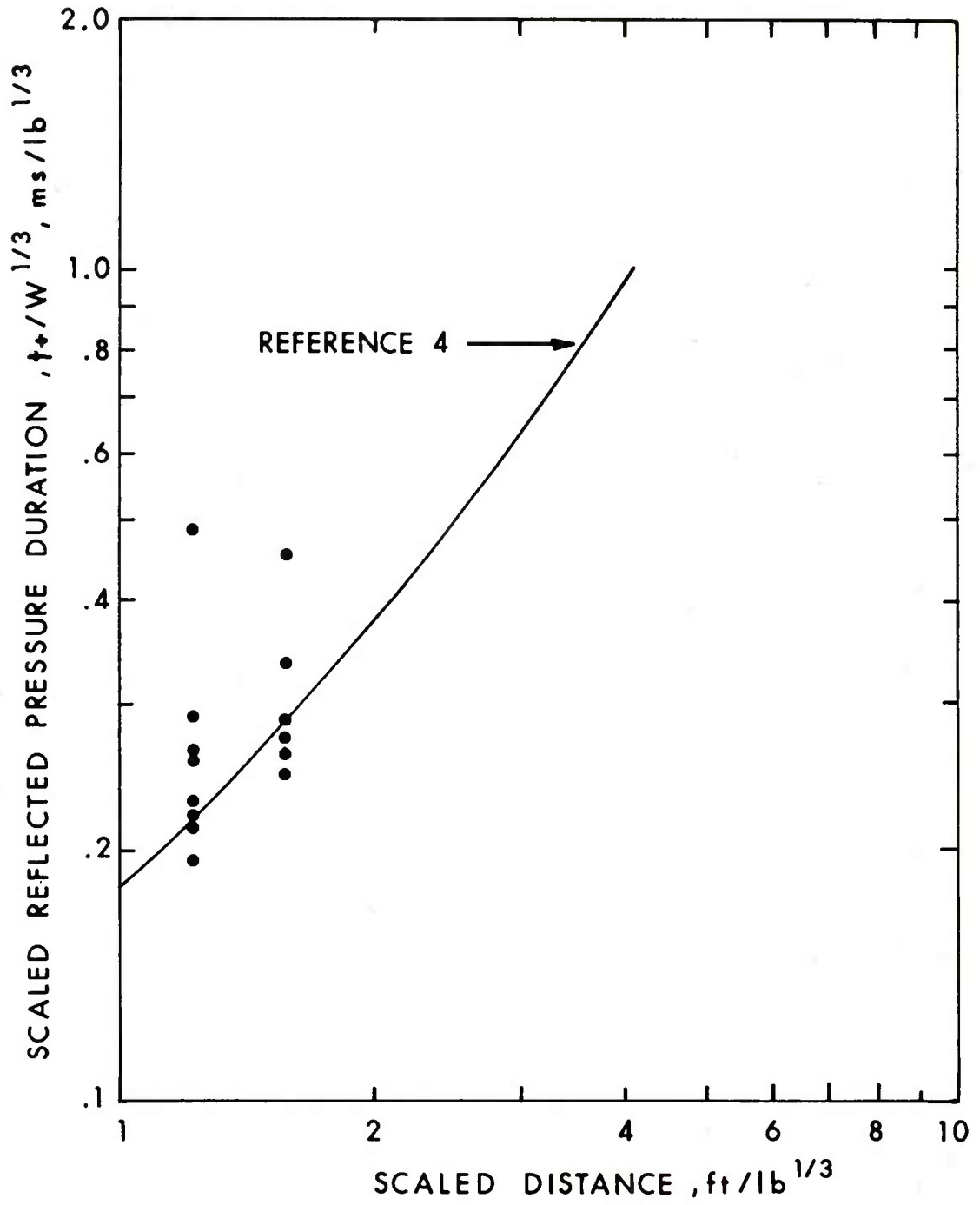


Figure 9. Scaled Reflected Pressure Duration versus Scaled Distance

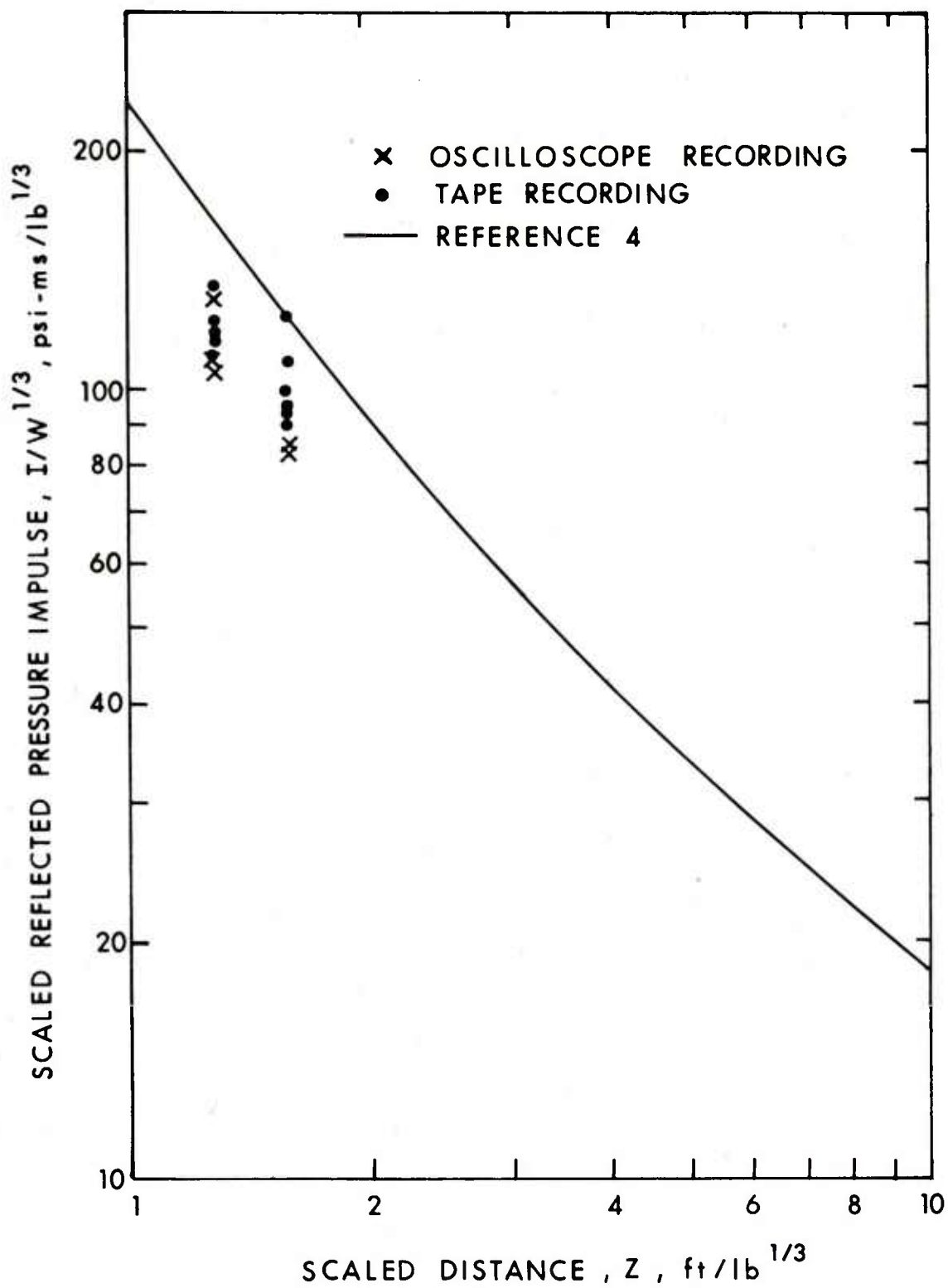


Figure 10. Scaled Reflected Pressure Impulse versus Scaled Distance

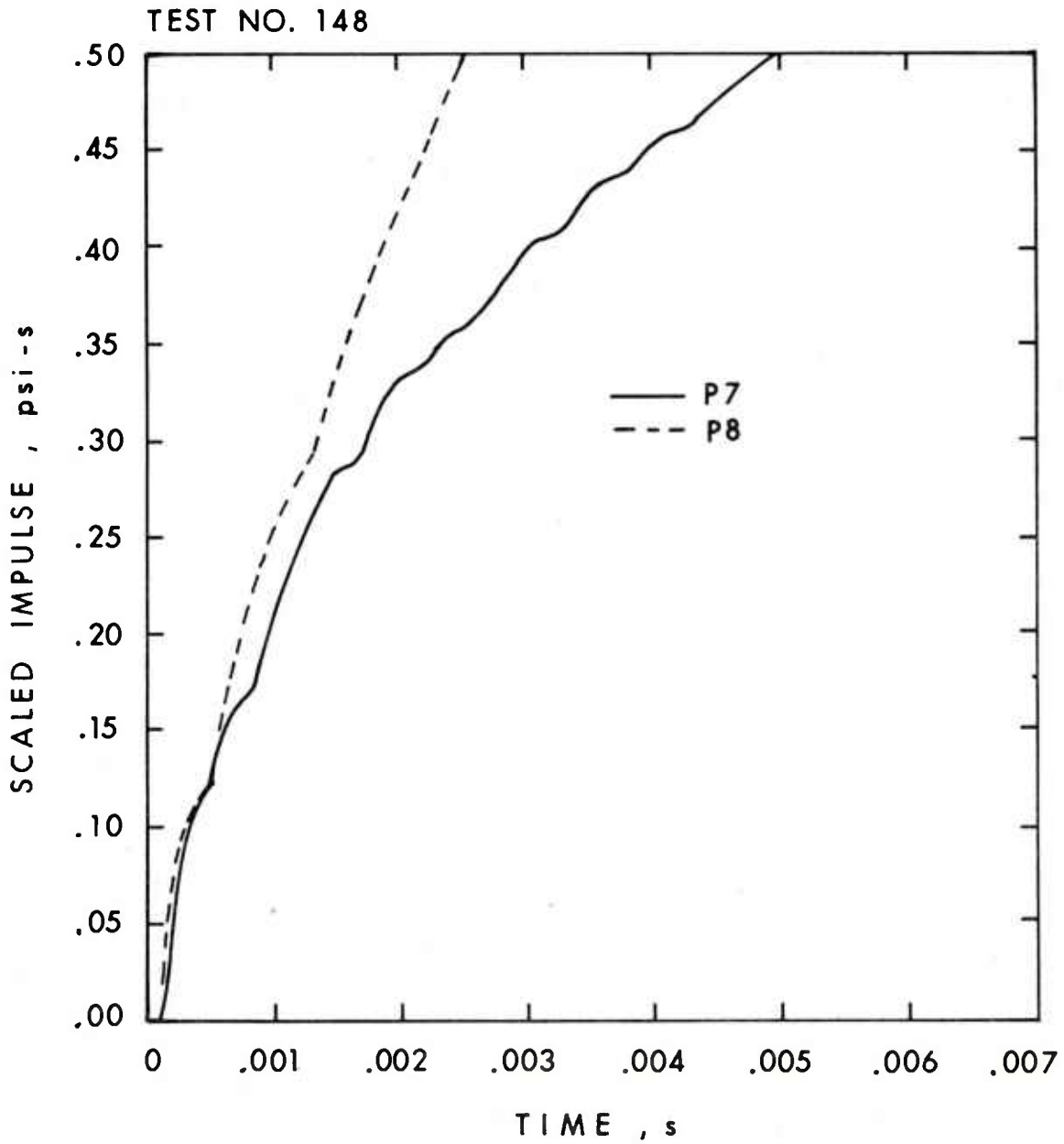


Figure 11. Reflected Impulse versus Time - P7 and P8 for T-5

TEST NO. 157

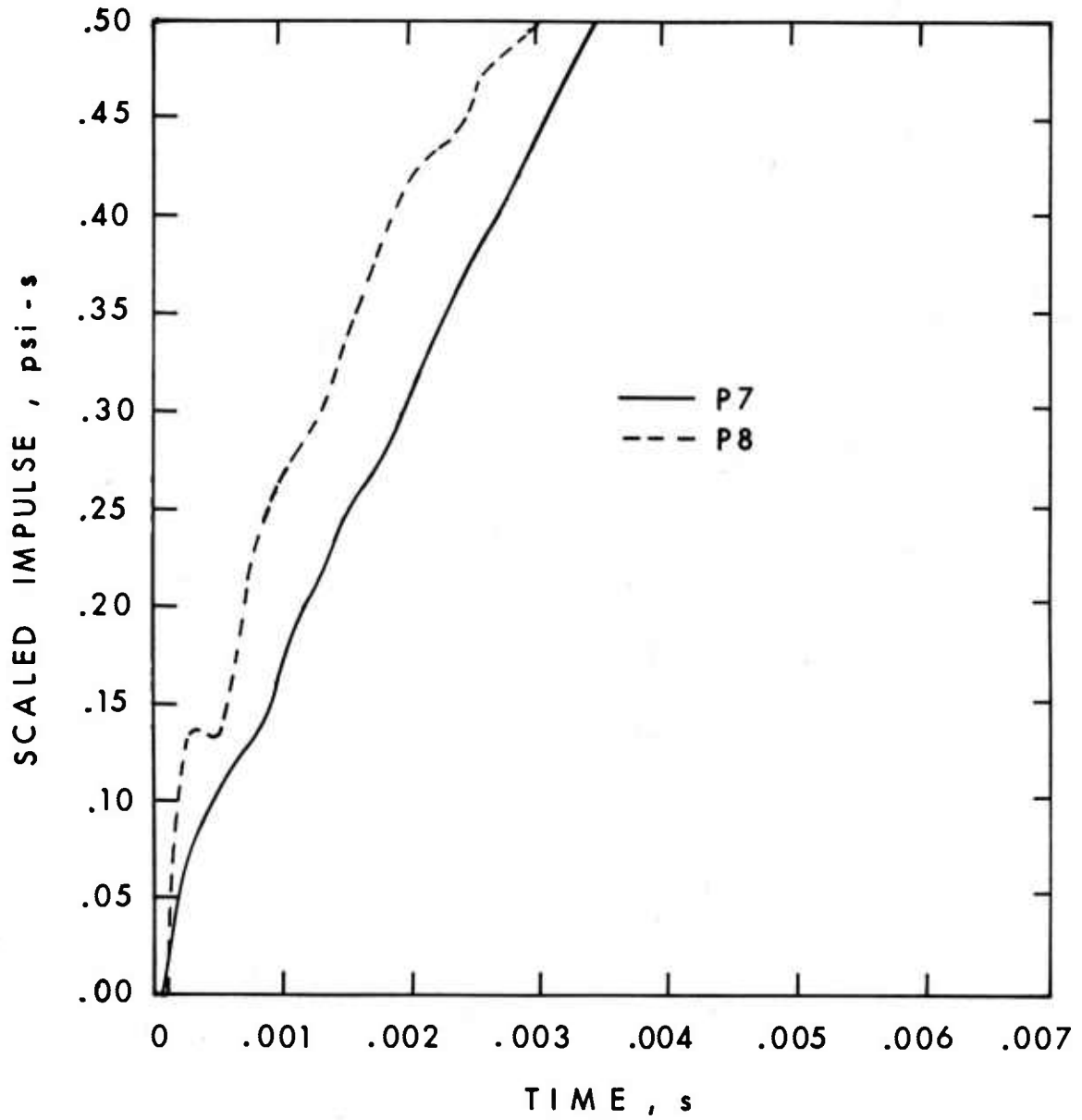


Figure 12. Reflected Impulse versus Time - P7 and P8 for 0-2

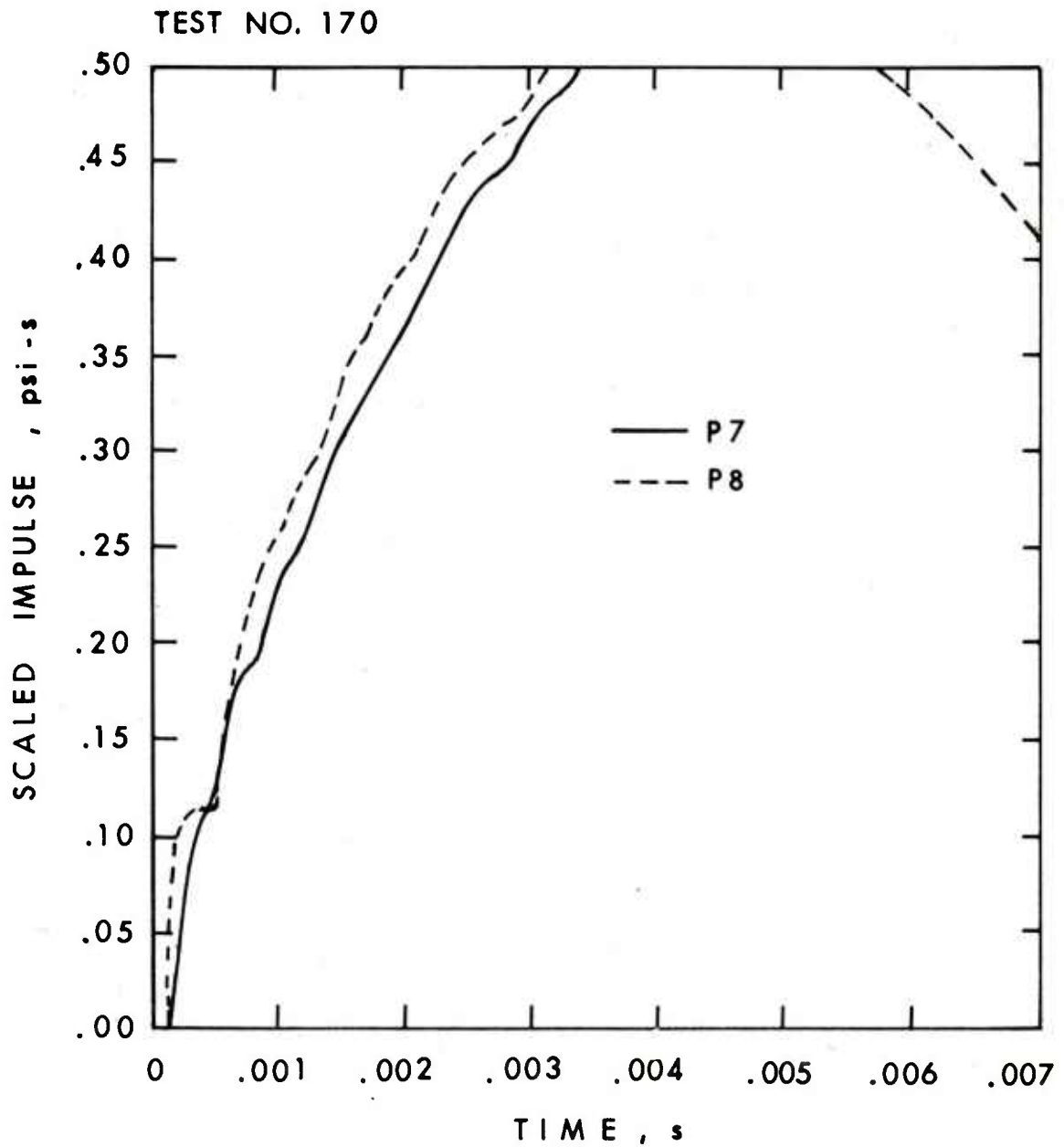


Figure 13. Reflected Impulse versus Time - P7 and P8 for 0-4

TEST NO. 173

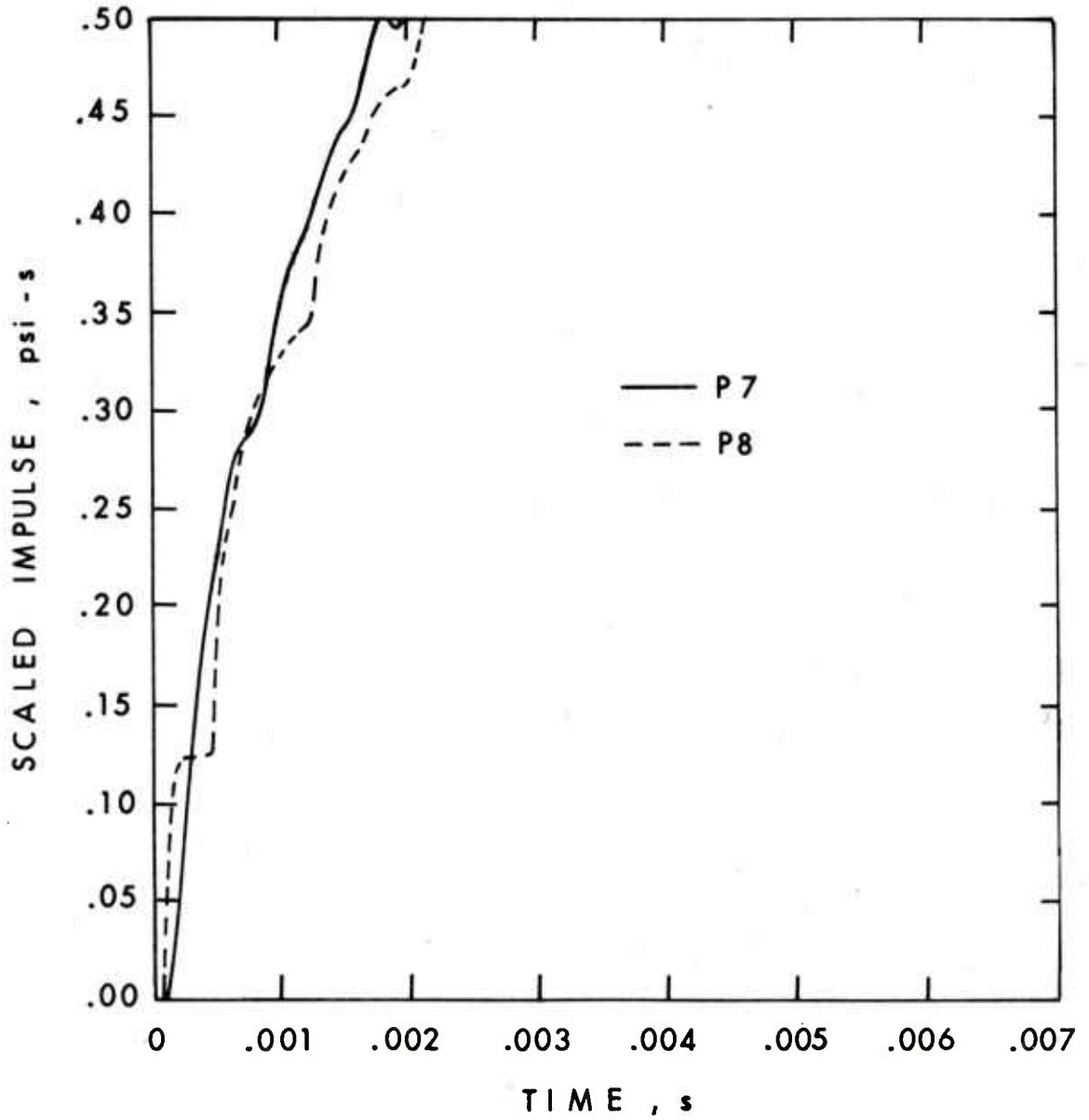


Figure 14. Reflected Impulse versus Time - P7 and P8 for NV

between gage locations P7 and P8. In general the impulse load is applied faster at location P8 than P7. The first plateau noted on the recorder from location P8 is the impulse in the first reflected shock on the side wall.

B. Quasi-Static Pressure Parameters

The quasi-static pressure is the term used to define the overpressure generated from the gaseous by-products when an explosion occurs in a closed or partially closed vessel. The magnitude of the quasi-static pressure is a function of the charge weight to structure volume ratio (W/V) (lbs./Ft^3). The duration of the quasi-static pressure is a function of the ratio of the vent area to volume of the structure (A_v/V) ($1/\text{Ft}$). On this series of tests the volume of the structure remained constant, 17.24 cubic feet. There were two charge weights, nominally 0.5 and 1.0 pounds. The effective vent area is the unknown parameter and an attempt will be made to determine it for each structure using the recorded duration and impulse of the quasi-static pressure pulse and relating them to experimental results obtained from structures with known vent areas.

1. Peak Quasi-Static Pressure. Determining the peak quasi-static pressure requires a degree of interpretation which is quite subjective. The quasi-static pressure is generated while the repeated reflected shocks are still in evidence, and in the structures where the vented area is large, the decay of the reflected shock pressures is in progress while the gas pressure is still being generated. The surface roughness of the structure wall affects the magnitude of the reflected shocks which in turn appears to affect the magnitude of the quasi-static pressure.

Two values of quasi-static pressure are listed in Table III. The first value P_{QE} is an extrapolation of the quasi-static pressure versus time back to a zero rise time. This method of extrapolation is shown in Figure 15 where the rate of decay of the quasi-static pressure due to venting is used to determine the value of P_{QE} . A second value of quasi-static pressure noted as P_{QA} is also listed in Table III. This is an average value determined at time of t equal to $W^{2/3}$, where W is the weight of the explosive charge in pounds and t is the time in milliseconds. This second value should be the maximum gas pressure prior to any decay due to venting. An example of the method used to determine the value P_{QA} is shown in Figure 15. The two values of peak quasi-static pressure listed in Table III are average values recorded at position 9.

Averages of the extrapolated values of quasi-static pressure (P_{QE}) listed in Table III are plotted in Figure 16 versus the charge weight to structure volume ratio. There is excellent correlation in

Table III. Quasi-Static Pressure Parameters

Charge Weight lbs	Structure							Avg	
	T-1	T-3	T-5	0-1	0-2	0-3	0-4		NV
	Pressure (psi) - Extrapolated (P_{QE})								
0.5	227	210	210	170*	190*	210	210	-	213
1.0	320	315	320	250	290	310	313	-	316
	Pressure (P_{QA}) psi at $t = W^{2/3}$ msec								
0.5	153	152	155	115*	115*	140	142	155	150
1.0	205	210	200	180	190	195	200	197	201
	Pressure Duration (t_g) ms								
0.5	7.0	10.5	15.0	44.0	36.0	28.0	15.0	-	
1.0	6.8	10.5	14.0	45.0	36.0	30.0	18.0	-	
	Pressure Impulse (I_g) psi-ms								
0.5	380	393	659	1480	1140	1100	680	-	
1.0	443	510	807	1930	1757	1880	1003	-	

* Not used in average

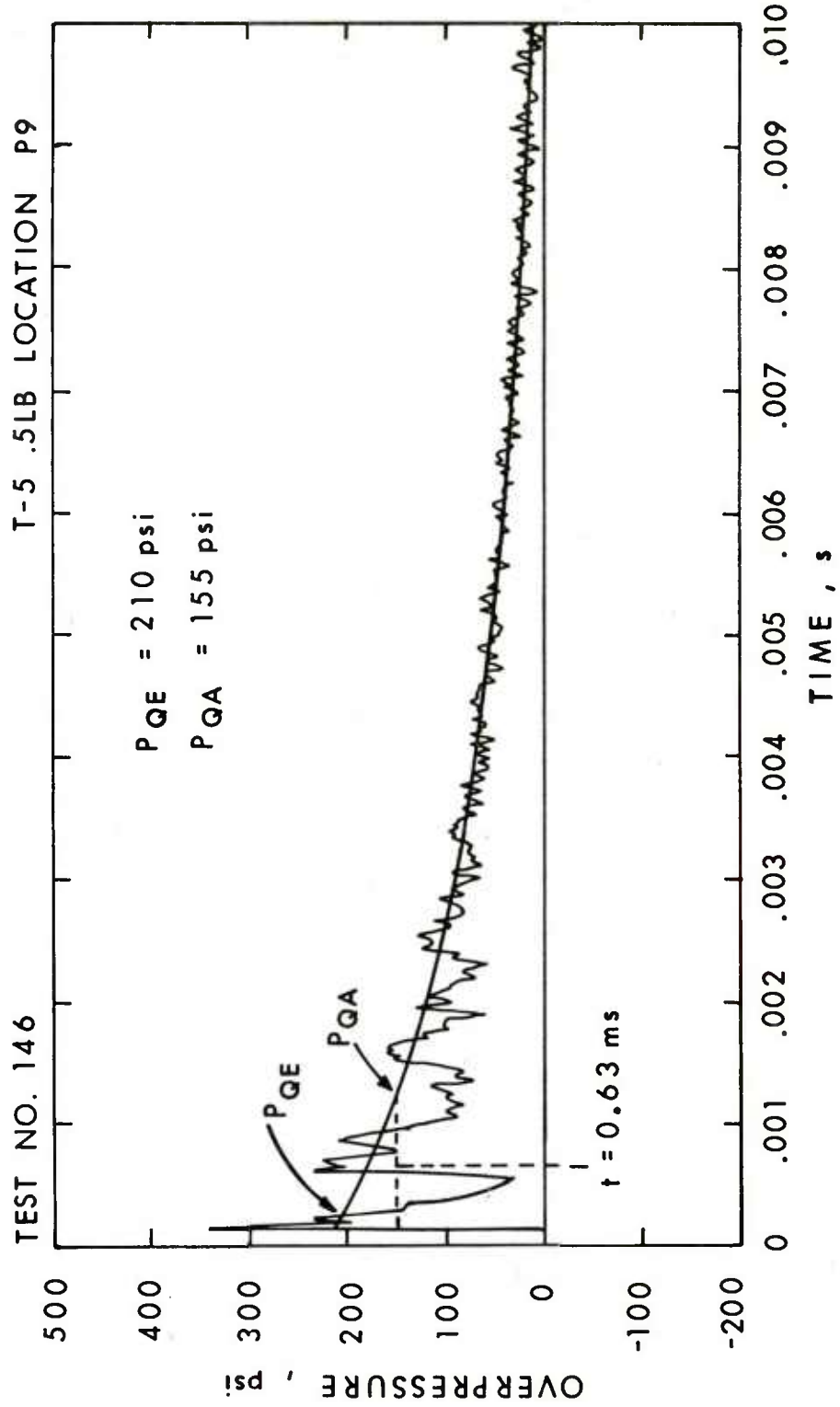


Figure 15. Method of Determining P_{QE} and P_{QA}

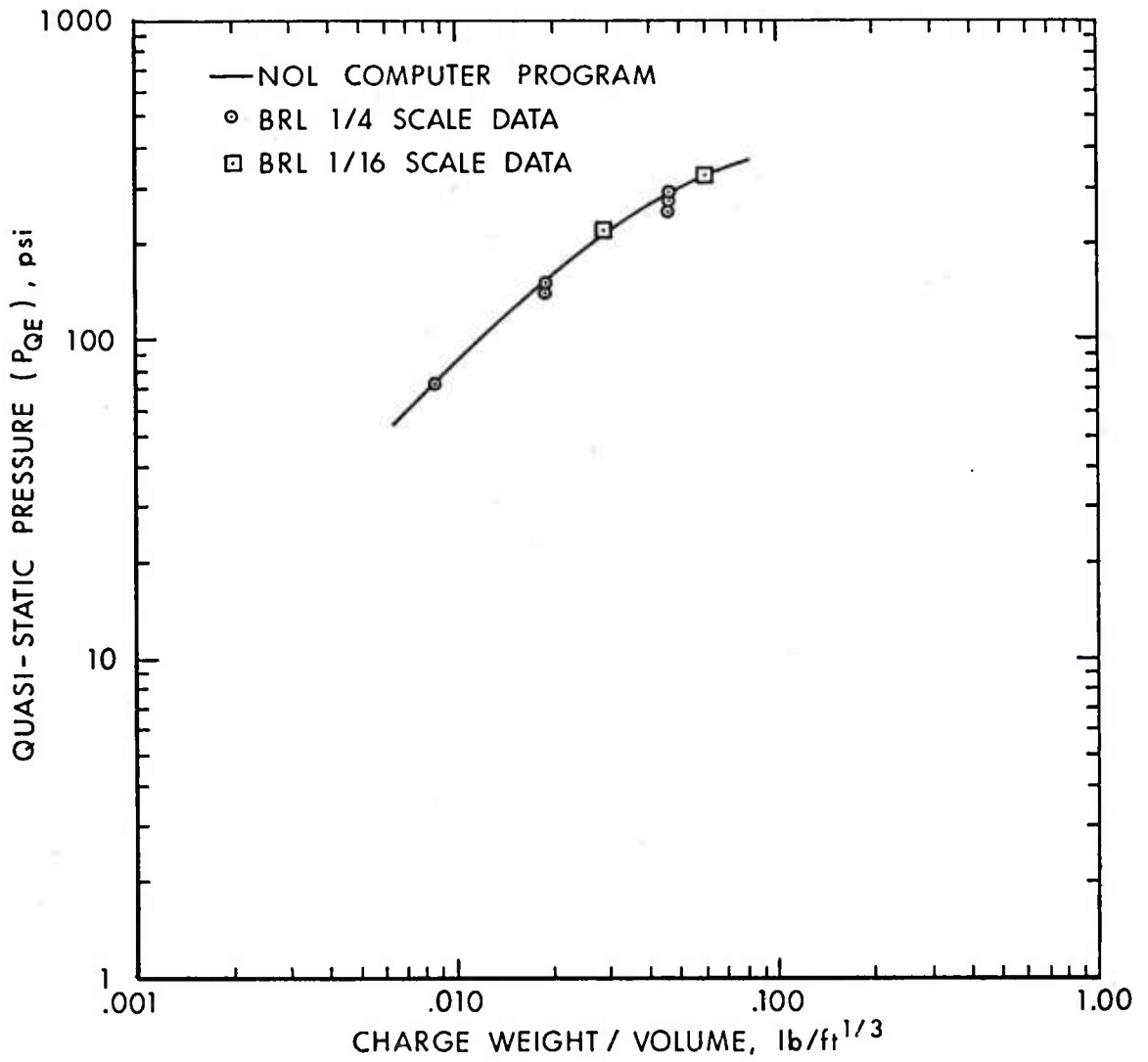


Figure 16. P_{QE} versus Charge Weight to Structure Volume Ratio

the values of P_{QE} recorded in all structures except 0-1 and 0-2. These two structures had the angle irons on the inner surface giving an extremely rough surface which lowered the peak reflected values thereby lowering the extrapolated value P_{QE} . Values of P_{QE} from structures 0-1 and 0-2 were not used and an average value of 213.4 psi was obtained for the 0.5 pound charge and 316 psi was obtained for the 1.0 pound charges. These values show excellent agreement with those obtained from Proctor's INBLAST computer code described in Reference 5. Also plotted in Figure 16 are values obtained from the 1/4 scale Category I testing, reported in Reference 6.

The method of determining P_{QA} is shown in Figure 15. The average values determined for each structure and for the two charge weights are listed in Table III. Here again the quasi-static pressures measured in structures 0-1 and 0-2 were considerably lower than the other structures and were not included in the final average. The final P_{QA} values determined were 150 psi for the 0.5 pound charges and 201 psi for the 1.0 pound charges. The two quasi-static pressure values (P_{QA}) are plotted in Figure 17 are data from the 1/4 scale Category I structure tests and test data from Naval Ordnance Laboratory and Naval Civil Engineering Laboratory reported in Reference 7. The data from this series of tests are in excellent agreement with other reported experimental results.

2. Quasi-Static Pressure Duration. The duration (t_g) of the quasi-static pressures recorded for each structure and charge weight are listed in Table III. The duration (t_g) in a suppressive structure is a function of the charge weight and the area vented (A_v) or A effective. The measured duration will be used in a later section to determine the effective vent area using different published methods in which the known vent areas were correlated with duration of the quasi-static pressure. When determining the quasi-static pressure duration it is difficult to interpret the exact time at which the overpressure returns to the ambient condition. From Table III it can be seen that there is little difference in the duration, t_g , for a 0.5 pound charge and a 1.0 pound charge detonated in the same volume structure with the same venting characteristics.

⁵Proctor, J. and Lorenz, R. A., "Internal Blast Computer Program," NSWC/WOL TR 75-183 (To be published).

⁶Schumacher, R., Kingery, C., and Ewing, W. Jr., "Airblast and Structural Response Testing of a 1/4 Scale Category I Suppressive Structure," BRL Memo Report.

⁷Minutes of the Fourteenth Explosives Safety Seminar, Keenan, W. A. and Tancreto, J. E., "Effects of Venting and Fragibility on Blast Environment from Explosions in Cubicles," pp 125 - 161, Nov. 1973.

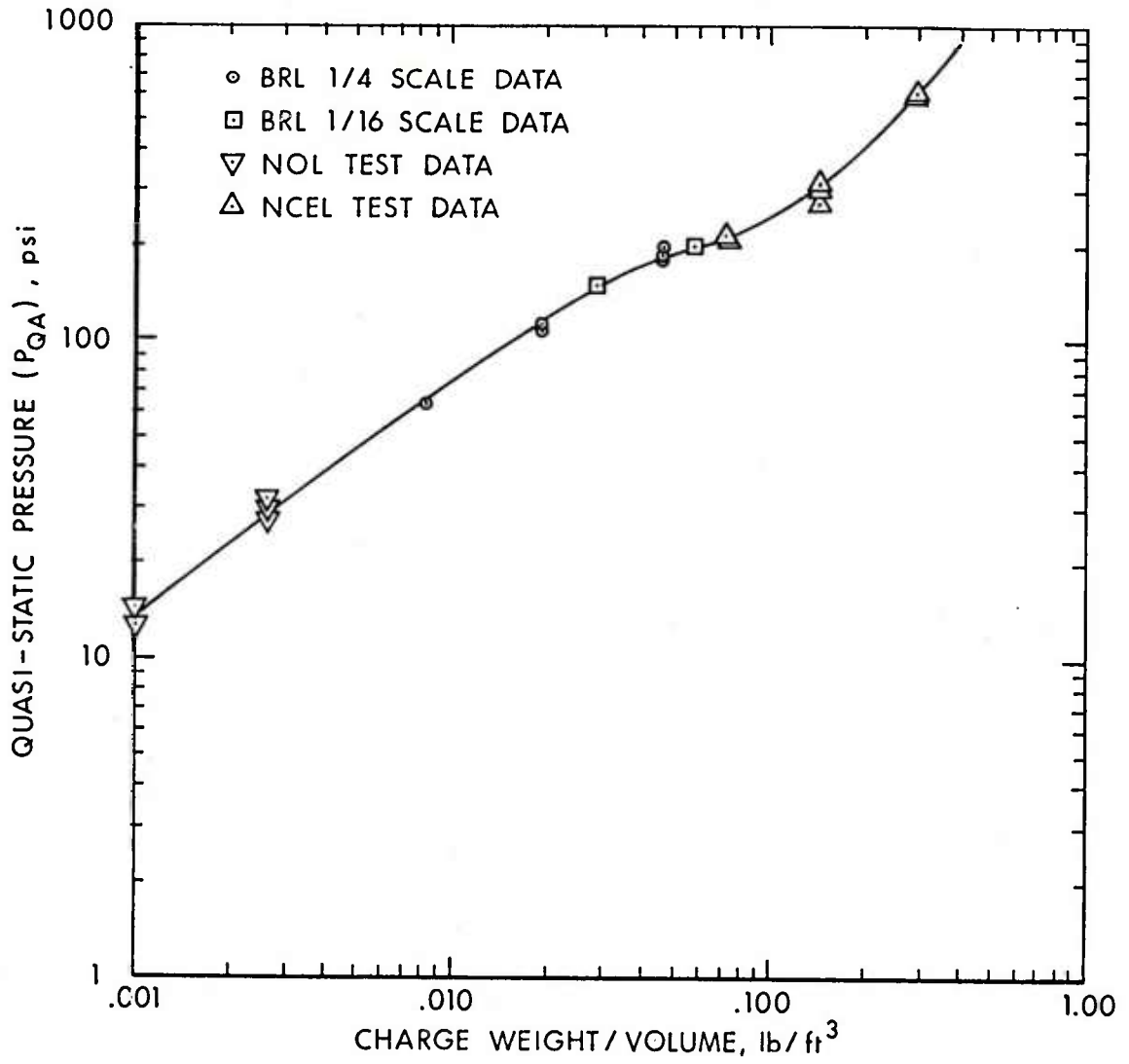


Figure 17. P_{QA} versus Charge Weight to Structure Volume Ratio

3. Quasi-Static Pressure Impulse. The quasi-static pressure impulse (I_g) was calculated from the records obtained at gage position P9 for all structures and charge weights. The average values are listed in Table III. The impulse (I_g) is a function of both the charge weight to structure volume ratio and the effective vent area. Since the effective vent area is an unknown parameter the measured impulse (I_g) will be used to infer the vent area, using relationships developed in Reference 8. It should be noted that the magnitude of the impulse (I_g) listed in Table III tends to increase as the calculated effective vent areas from Table I decreases.

C. Effective Vent Area

In any containment type structure the amount of venting has an effect on both internal and external pressure. The relationship between the effect of venting on internal and external pressure is discussed in Reference 5, 7, and 8 for known single vent areas. In this test series the four structure walls and roof were vented with the multilayer panels for which proven methods for determining the effective vent area have not been developed. The measured duration and impulse from these tests will be used in an attempt to determine an effective vent area by comparing them to published data relating to known vent areas.

1. Effective Vent Area from Quasi-Static Pressure Duration. The durations of the quasi-static pressure (t_g) are listed in Table III for each structure and two charge weights. These values will be used in four different methods to establish effective vent areas for each structure.

In Reference 1 a relationship was established by Southwest Research Institute (SwRI) showing that the quasi-static pressure duration could be described as

$$\frac{t_g}{P_{QA}^{1/6} V^{1/3}} = f \left(\frac{A_v^{3/2}}{V} \right) \quad (2)$$

Using Figure 6 in Reference 1 values of effective A_v were determined. These values are listed in data column one of Table IV. The curve presented in Reference 1 was extrapolated to smaller values of $t_g/P_{QA}^{1/6} V^{1/3}$ to accommodate the "T" type structures and structure 0-4.

⁸ Minutes of the Sixteenth Explosives Safety Seminar, Keenan, W. A. and Tancreto, J. E., "Blast Environment from Fully and Partially Vented Explosives in Cubicles," pp 1527 - 1559, September 1974.

Table IV. Effective Vent Area (Duration t_g)

Structure	Chg WT Pounds	SwRI A_{V2} FT ²	NCEL A_{V2} FT ²	NSWC A_{V2} FT ²	K&S A_{V2} FT ²	Average A_{V2} FT ²	Percent Area Vented
T-1	0.5	3.39	2.83	3.26	2.91	3.10	9.29
T-1	1.0	3.12	3.00	3.61	3.34	3.27	9.79
T-3	0.5	2.28	2.39	2.17	1.89	2.18	6.53
T-3	1.0	2.36	2.60	2.34	2.16	2.37	7.10
T-5	0.5	1.62	1.84	1.52	1.32	1.58	4.73
T-5	1.0	1.86	2.07	1.75	1.62	1.81	4.85
0-1	0.5	.458	.526	.519	.419	.481	1.44
0-1	1.0	.475	.532	.546	.468	.505	1.51
0-2	0.5	.571	.664	.634	.533	.601	1.80
0-2	1.0	.630	.690	.682	.613	.654	1.96
0-3	0.5	.806	.889	.816	.709	.806	2.42
0-3	1.0	.794	.852	.819	.751	.804	2.41
0-4	0.5	1.67	1.84	1.52	1.32	1.59	4.76
0-4	1.0	1.43	1.54	1.36	1.25	1.40	4.19

Area of vented walls = 33.37 FT²

Percent of vent area = $\frac{\text{vent area}}{33.37} \times 100$

An extensive series of tests was conducted by Kennan and Tancreto of the Naval Civil Engineering Laboratory in an effort to relate the duration of the quasi-static pressure (t_g) and the area vented A_v . This work is reported in Reference 8. An equation was developed where

$$t_g/W^{1/3} = 2.26 (A_v W^{1/3}/V)^{-0.86} \quad (3)$$

This equation is valid for $A_v/V^{2/3} < 0.21$ which means the vent area should be less than 1.4 ft^2 for this equation to be valid. For vent areas greater than this a family of curves presented in Reference 8 was used. The values obtained from the curves and equation are listed in data column 2 of Table IV.

A third method used for calculating the effective vent area from the measured quasi-static duration (t_g) is based on a family of curves developed by Proctor of the Naval Surface Weapons Center (NSWC) and published in Reference 9. In Figure 9 of Reference 9 curves of scaled duration $t_g/W^{1/3}$ versus scaled venting $(V/A_v)/W^{1/3}$, for different charge weight to structure volume ratios are presented. Based on these curves, a simple equation was established for the two charge weight to structure volume ratios; i.e., 0.029 for the 0.5 pound charge and 0.058 for the 1.0 pound charge. The equation is

$$A_v = \frac{K V}{t_g} \quad (4)$$

where

$$K = 1.375 \text{ ms/ft for } W/V = 0.029 \text{ lb/ft}^3$$

$$K = 1.425 \text{ ms/ft for } W/V = 0.058 \text{ lb/ft}^3.$$

The effective vent area A_v was calculated for each structure and charge weight and the values are listed in data column 3 of Table IV. There is good correlation between the three methods with no significant differences or trends noted.

⁹61-JTCG/ME-73-3 Joint Technical Coordinating Group for Munition Effectiveness, Proctor, J. F., "Internal Blast Damage Mechanism Computer Program," 10 April 1973.

A fourth method relating effective vent area to quasi-static pressure duration was developed by Kinney and Sewell and is reported in Reference 10. In this reference an equation was derived to describe the quasi-static pressure decay versus time.

$$\text{Log } P = \text{Log } P_{\text{max}} - .315 \left(\frac{A_v}{V} \right) t_s \quad (5)$$

where

P = absolute pressure in atmosphere

A_v = vent area - square meters

V = volume - cubic meters

t_s = time - milliseconds.

Arranging the terms to calculate A_v , when $t_s = t_g$ then $P = 1$ and the equation becomes

$$A_v = (\text{Log } P_{\text{max}}) (V) / .315 t_g \quad (6)$$

For these calculations the values for P_{QE} listed in Table III were used for P_{max} . A value of A_v was calculated for each structure and charge weight using the measured t_g listed in Table III. These values are listed in column four of Table IV and with the exception of structure T-1, the results are slightly lower than those calculated using the other three methods.

Average values for the four methods are listed in data column 5 for each structure and charge weight. There is excellent correlation between the two values of effective vent area established for each structure from the two charge weights. Using the relationship established in Equation 4 two solid lines are drawn in Figure 18 for the two charge weight to volume ratios. The data points are the average values from data column 5 shown in Table IV.

2. Determining Effective Vent Area from Quasi-Static Pressure Impulse. The primary source of information relating the quasi-static pressure impulse (I_g) to known vent areas and charge weight to structure

¹⁰ Kinney, G. F. and Sewell, R. B. W., "Venting of Explosives," NWC Tech Memo 2448, July 1974.

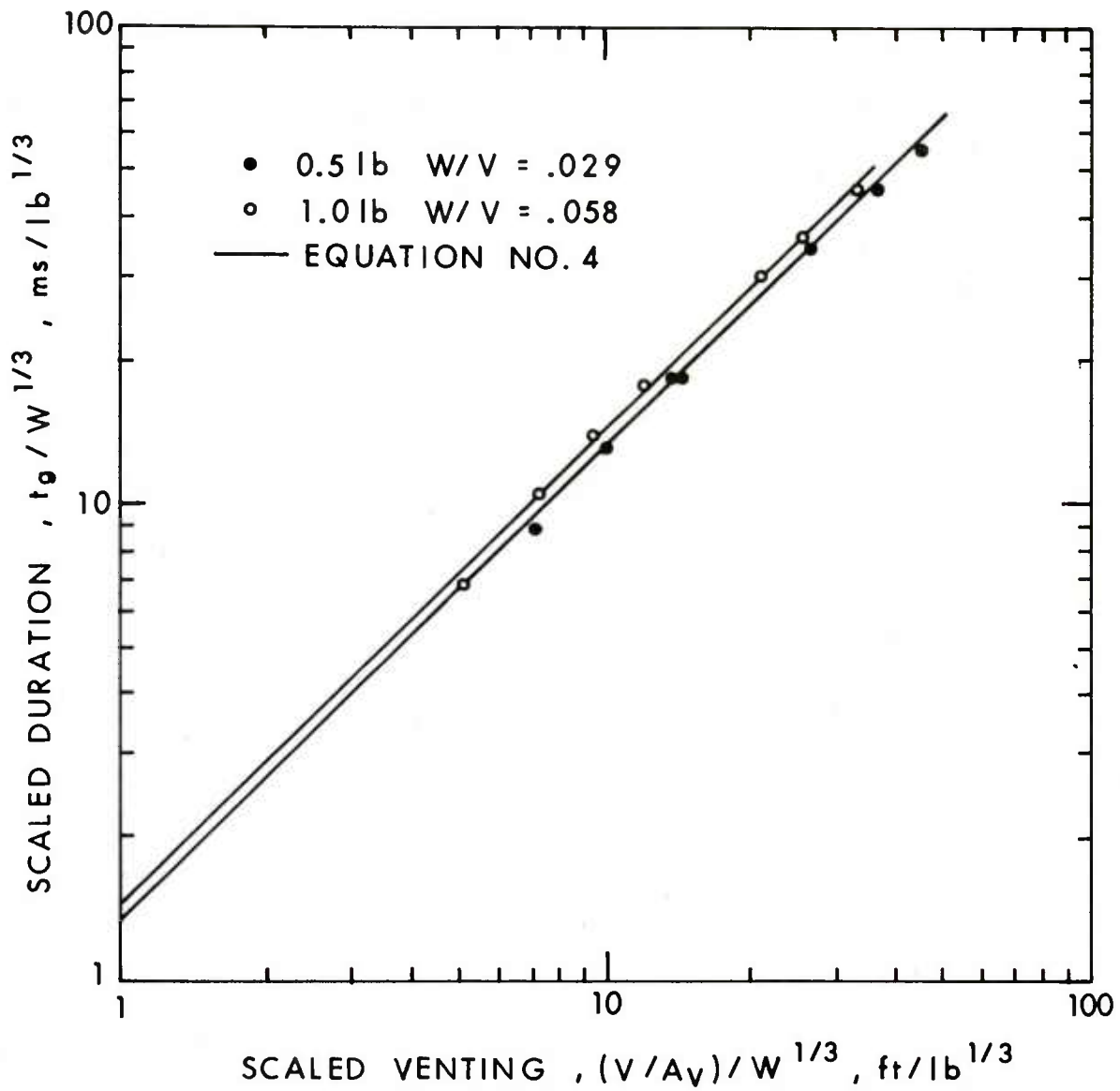


Figure 18. Scaled Venting $(V/A)/w^{1/3}$ versus Scaled Duration $t_g/w^{1/3}$

Table V. Effective Vent Area - Impulse I_g

Structure	Chg WT Lbs	I_g psi-ms	A_v
T-1	0.5	380	2.77
T-1	1.0	443	2.80
T-3	0.5	393	2.64
T-3	1.0	510	2.60
T-5	0.5	659	2.18
T-5	1.0	807	2.56
0-1	0.5	1480	.772
0-1	1.0	1930	.838
0-2	0.5	1140	1.07
0-2	1.0	1757	.943
0-3	0.5	1100	1.13
0-3	1.0	1880	.865
0-4	0.5	680	2.09
0-4	1.0	1003	1.94

volume ratios is published in Reference 8. In this reference an equation was developed which is valid for $A_v/V^{2/3} < 0.21$. The equation is

$$I_g/W^{1/3} = 569 (A_v/W^{2/3})^{-.78} (W/V)^{-.38}. \quad (7)$$

For $A_v/V^{2/3}$ greater than 0.21 there is a family of curves from which A_v can be determined if I_g is known. The equation and curves were used to determine the effective vent area of the seven vented structures. The values determined by this method are listed in Table V. The correlation of effective vent areas determined from the impulse (I_g measurements and duration (t_g) measurements) is only fair. The impulse (I_g) determinations of the effective vent area are larger than those determined from the duration (t_g) with the exception of structure T-1. One reason suggested for the difference in the two is that the filtering of the record in recording the quasi-static pressure versus time may have inferred smaller values of impulse and thus larger vent areas. It is suggested that the effective vent areas (A_v) determined from the duration t_g data be utilized and less reliance placed on those determined from the impulse data.

D. Internal Pressure Loading

The pressure loading the walls of the 1/16 size structure is a combination of repetitive reflected shocks and the gas pressure generated by the explosive. The records presented in this section will show the reflected shocks and while the time of occurrence is accurate the pressure magnitude is not. This is because the signal was filtered in order not to overdrive the recording system. The primary interest was in the quasi-static pressure which is always much lower than the reflected pressures.

The magnitudes of the repeated reflected shocks are affected by the type of interior surface of the wall panel. The rate of decay of the quasi-static pressure is of course a function of the effective vent area.

1. Internal Pressure in Structures T-1, T-3, and T-5. A sketch of the construction of the "T" type structure (Interlocking I-Beams) panels is presented in Figure 1a. It should be noted that the wall thickness remained the same and the different effective vent areas were obtained by changing the dimensions of E or the separation of the I-Beam flanges.

In Figure 19 the internal pressure versus time recorded on the center of the wall of structures T-1, T-3, and T-5 is presented for the first .01 second. The first peak reflected pressure should be ignored

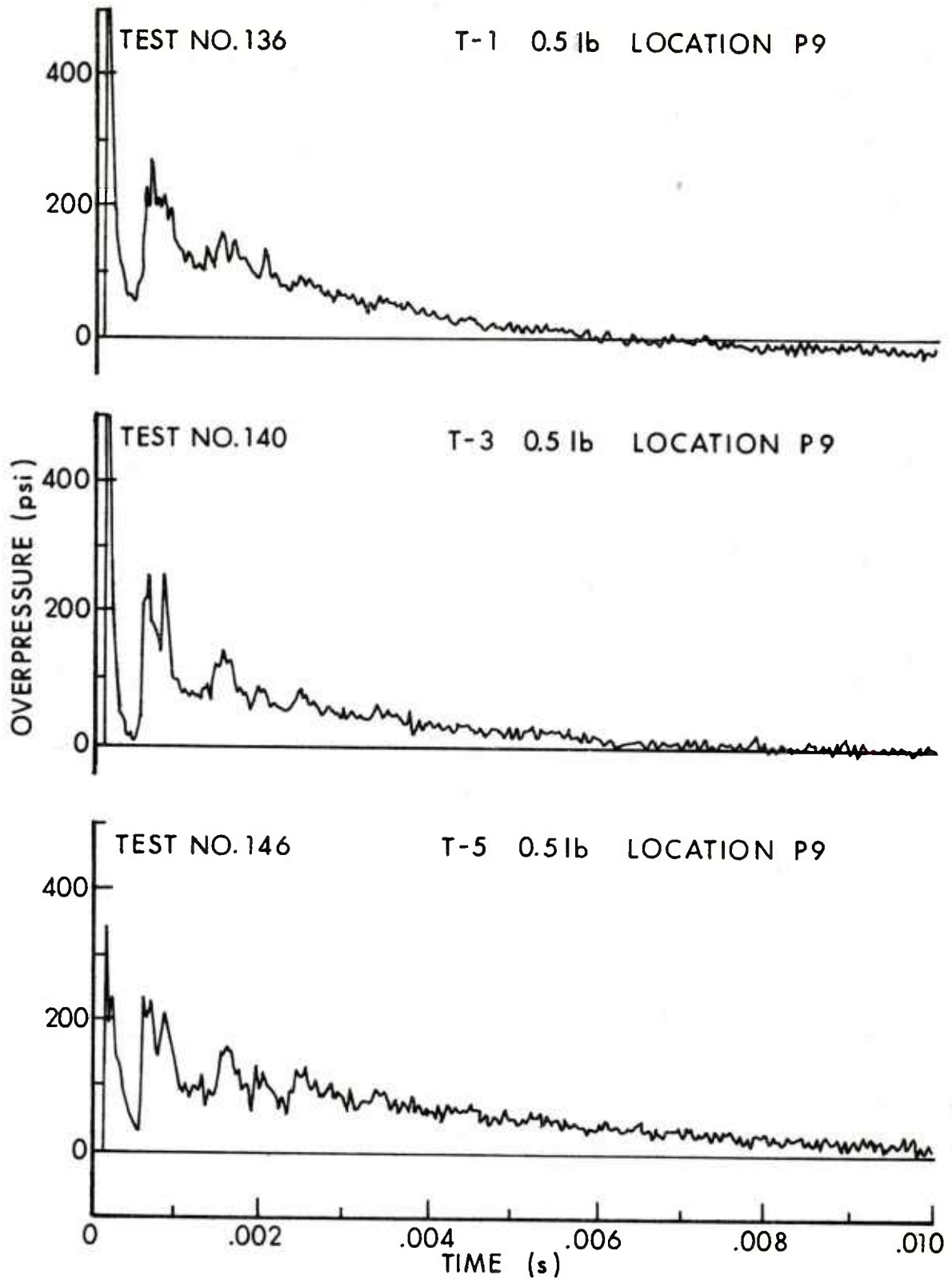


Figure 19. Internal Pressure versus Time at P9 in Structures T-1, T-3, and T-5, 0.5 Pound Charge

because it has been allowed to overshoot the recording system as shown on records from T-1 and T-3 and it has been filtered out in the data processing as shown on the record from T-5. The pressures reflected from the walls converge back to the center of the structure and then reflect outward again. This process is repeated a number of times with the reflected pressure impinging on the wall decreasing in magnitude each time.

It should be noted in Figure 19 that in all three structures the first pressure reflection after the decay of the peak reflected pressure is approximately the same magnitude and occurs at the same time. The magnitude of this outward reflected pressure recorded on a non-filtered high response gage is approximately 500 psi rather than 250 psi as shown on the records in Figure 19.

As the vent area is decreased in going from T-1 to T-3 to T-5 the rate of decay of the internal pressure is decreased and duration is increased.

In Figure 20 the time scale has been compressed to show the total duration of the pressure pulse recorded in structure T-5 at Position 9.

2. Internal Pressure in Structures 0-1, 0-2, and 0-3. The walls of structures designated 0-1, 0-2, and 0-3 were comprised of different panel elements as shown in Figure 1b but were predicted to have the same venting and attenuation characteristics. In structure 0-1 the wall consists of one layer of closely spaced angle iron and two perforated plates. In structure 0-2 the angle iron is larger and wider spaced and there are three perforated plates. The 0-3 structure wall had four perforated plates. They were off-set so that the holes did not fall in line.

The internal pressure versus time during the first .01 second in structures 0-1, 0-2, and 0-3 is shown in Figure 21. The rate of decay of internal pressure in the three structures appears quite similar in that they show approximately the same overpressure at .01 seconds. The first pressure reflection after the peak value is lower in structure 0-1 than in structure 0-2 and also lower in structure 0-2 than in structure 0-3. The magnitudes of these reflections are a function of the initial reflected wave on the wall surface and the outward reflection from the center of the structure. The wall panel in structure 0-1 has small closely spaced angle irons (Figure 1b) which apparently disturb the formation of the peak reflected pressure on the wall causing a lowering of the outward reflection from the center of the structure. Note record from structure 0-1 in Figure 21.

The wall panel of structure 0-2 is shown in Figure 1b. The larger angle irons and wider spacing apparently produce a higher reflected pressure than structure 0-1. Therefore, the first outward reflected wave in structure 0-2 as shown in Figure 21 is of greater magnitude than that of structure 0-1.

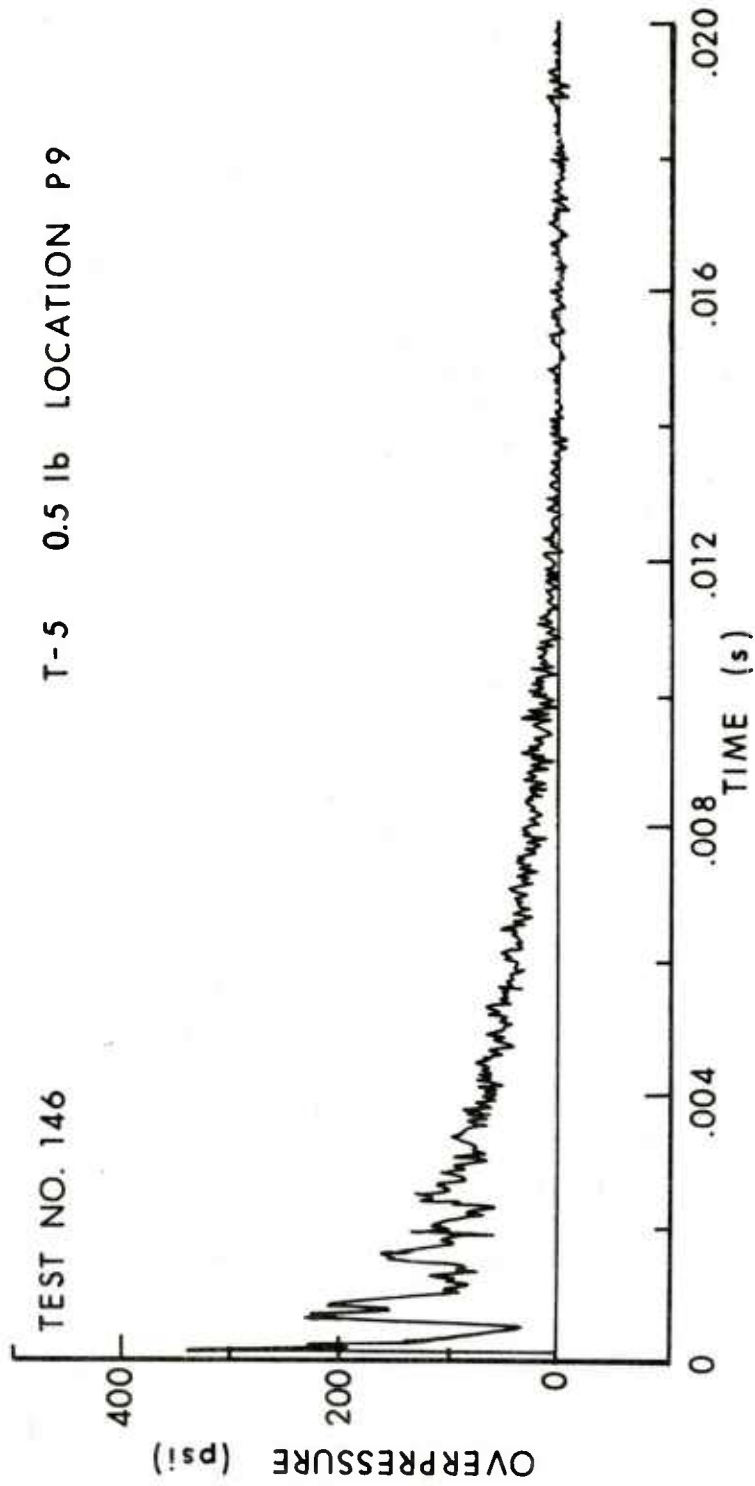


Figure 20. Compressed Time Scale Showing Complete Pressure Pulse for T-5

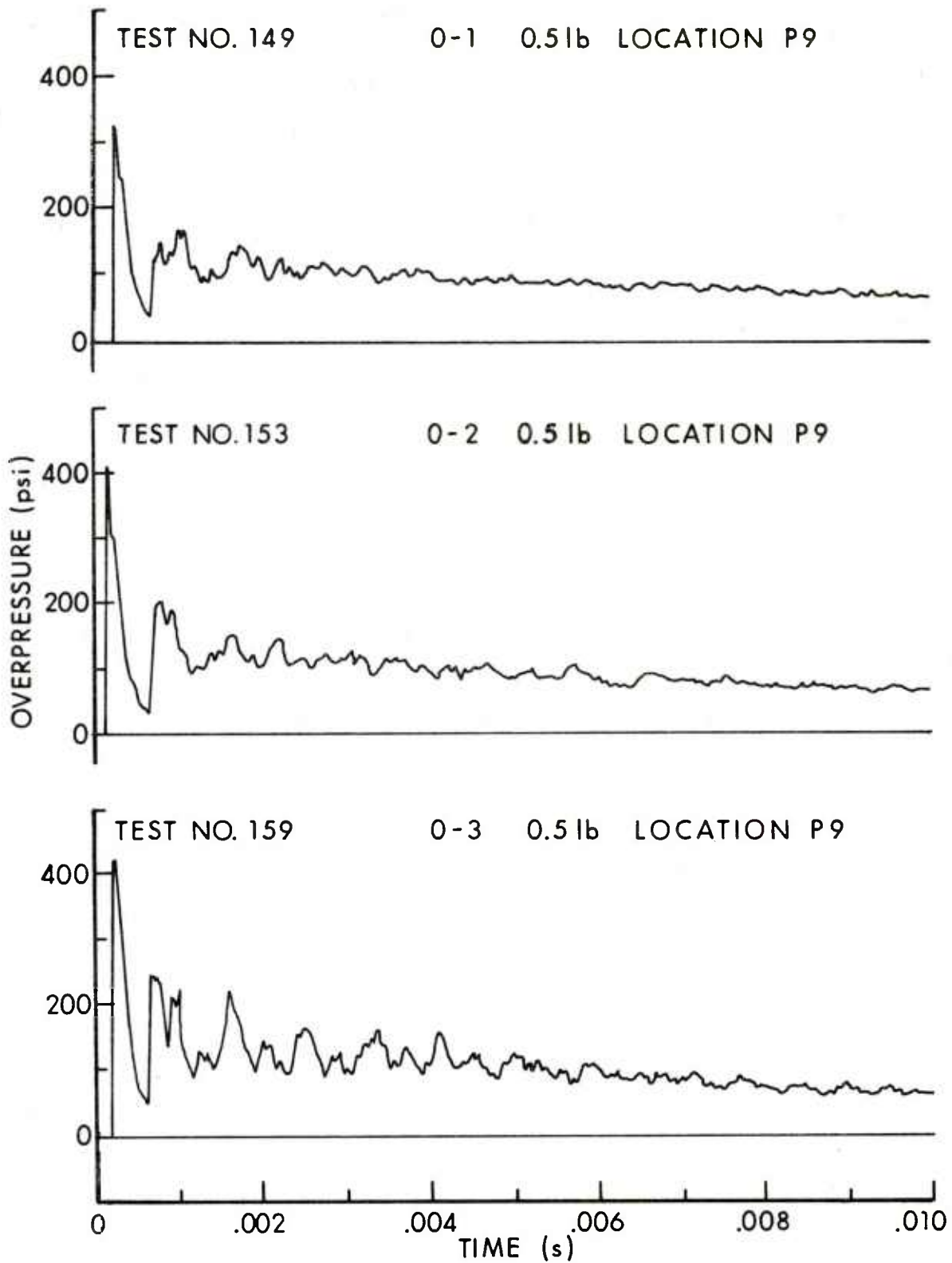


Figure 21. Internal Pressure versus Time at P9 in Structures 0-1, 0-2, and 0-3, 0.5 Pound Charge

Since structure 0-3 has a wall of perforated plate, the second shock reflection on the wall would be expected to be greater than those recorded in structures 0-1 or 0-2. This is recorded in Figure 21. Here it should be noted again that comparisons are between relative magnitudes of the outward reflected pressures and are not quantitative. The magnitude of the reflected wave in structure 0-3 is approximately the same as that recorded in the type "T" structures which also have relatively flat walls.

The total pressure durations of the records presented in Figure 21 are shown in Figure 22 with a compressed time scale. Although the overpressure was approximately the same at a time of .010 seconds, the pressure decay rate at times greater than .010 seconds as well as the total duration are different. Structure 0-1 has a slower decay rate and longer duration than structure 0-2 which implies less effective venting than structure 0-2. Structure 0-2 has a slower pressure decay rate and longer duration than structure 0-3 which implies that structure 0-2 has less effective venting than structure 0-3. Although planned to have the same effective venting characteristics based on the method discussed earlier, the three structures have three different effective vent areas (see Table IV).

3. Internal Pressure in Structure 0-4. Structure 0-4 was option 4. It consists of four perforated plates as shown in Figure 1b. The primary difference between structure 0-3 and structure 0-4 is the number of holes in the perforated plates. Structure 0-4 had almost twice as many holes per plate as structure 0-3 and was calculated to have the same effective vent area as structure T-5.

The internal pressure versus time recorded at P9 from the detonation of a 0.5 pound charge in structure 0-4 is presented in Figure 23. A similar record from structure T-5 is also presented in Figure 23 for comparison. It is quite clear from this comparison that the 0-4 structure does have a similar effective vent area as structure T-5, as predicted in Table 1 and determined in Table IV.

4. Internal Pressure in Structure N-V. Structure N-V was a solid wall box structure and the N-V designates non-venting. It had the same interior dimensions and volume as the other structures. It was manufactured from 3/4 inch steel plate. This configuration was utilized to determine the internal pressure on the wall of the structure as the vent area approached zero. Structure N-V approximated a non-venting structure but could not be completely sealed. The access door used for placement of the charge was close-fitting but not sealed, and a 1/8-inch hole was drilled through the center of the top plate for installation of the firing line.

The internal pressure versus time recorded at P9 from the detonation of a 0.5 pound charge in structure N-V is presented in Figure 24. The pressure is shown for 0.05 second and there has been a relatively small pressure decay during that time. The internal pressure decayed to

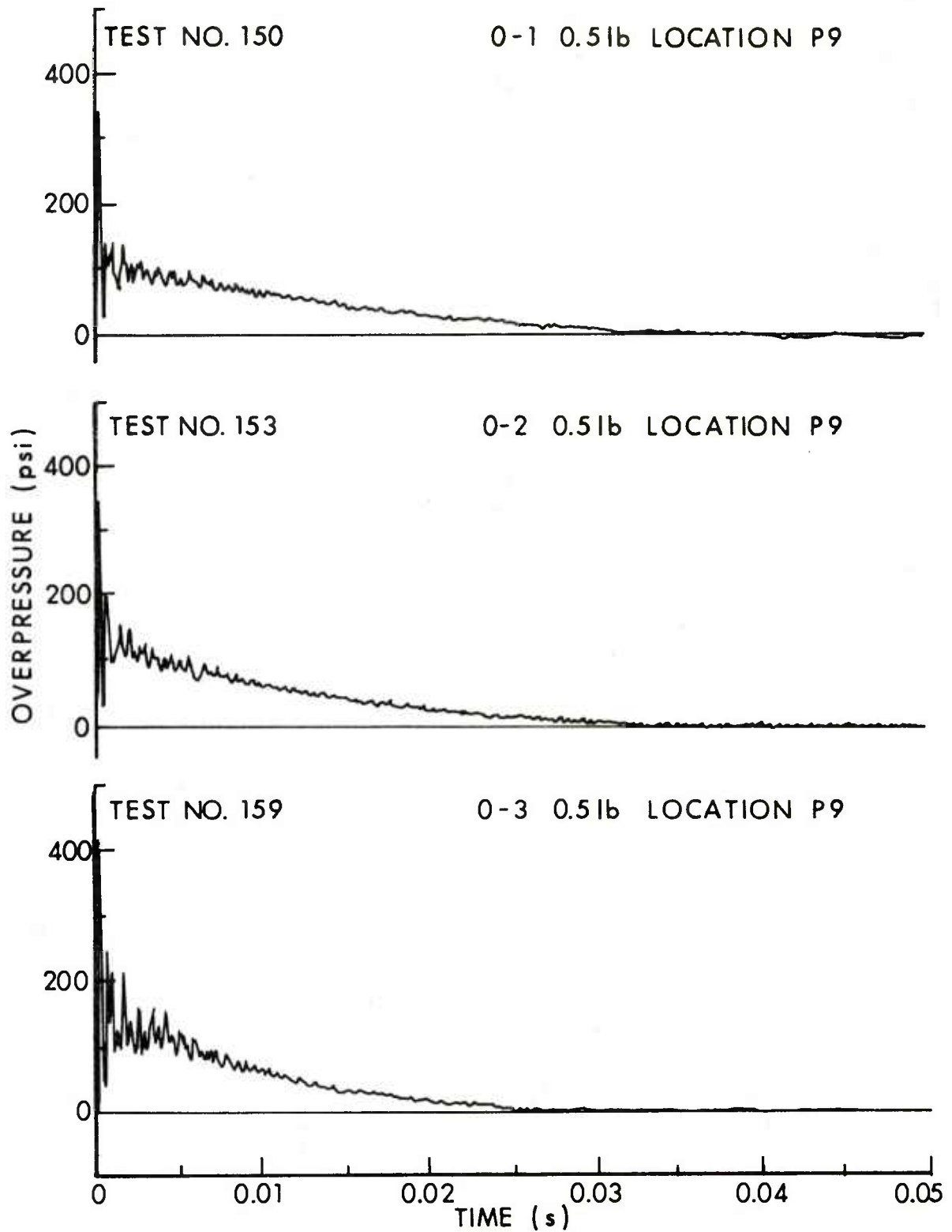


Figure 22. Compressed Time Scale Showing Complete Pressure Duration of Figure 21 Records

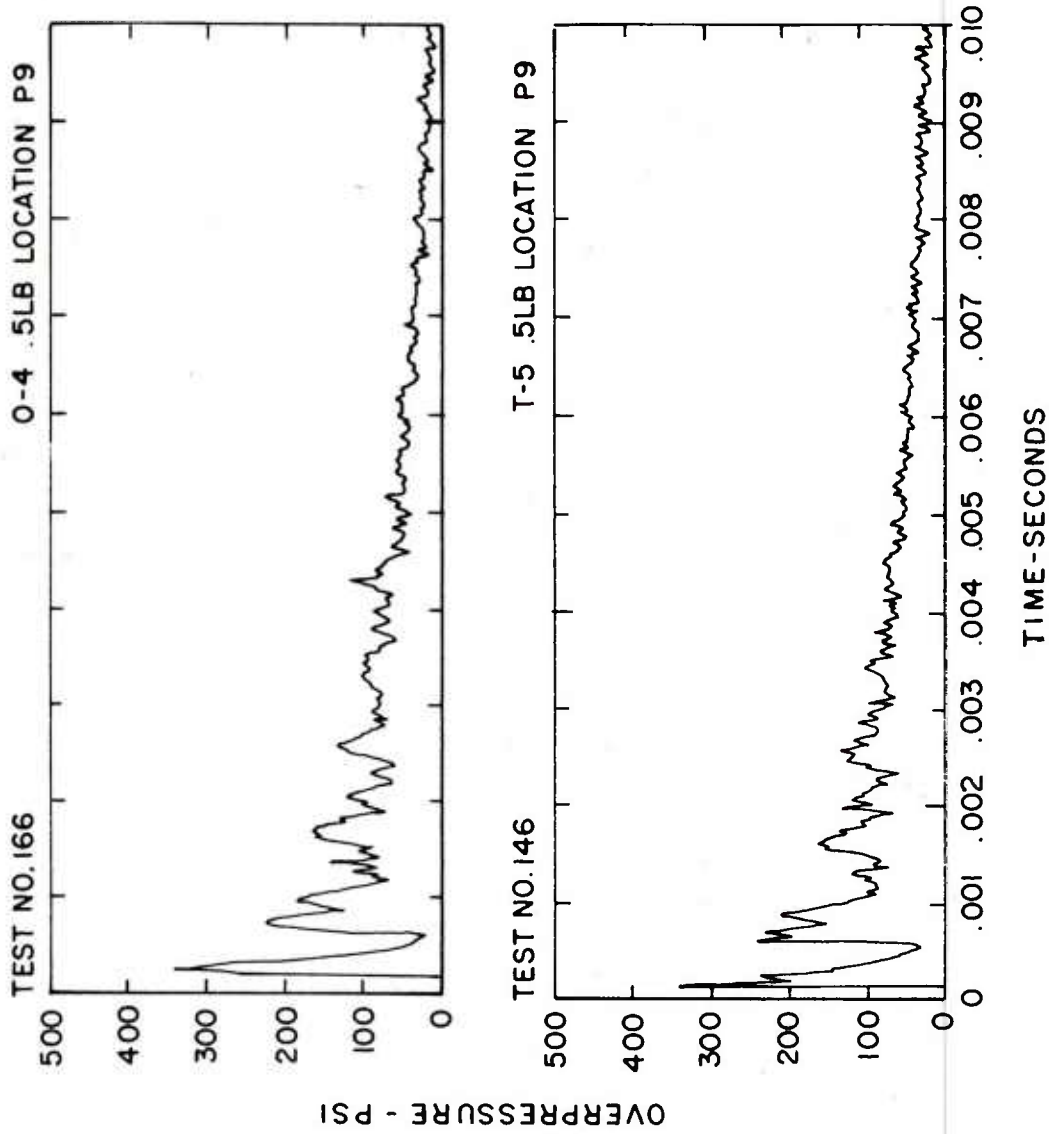


Figure 23. Comparison of Internal Pressure versus Time Recorded in Structure O-4 and Structure T-5

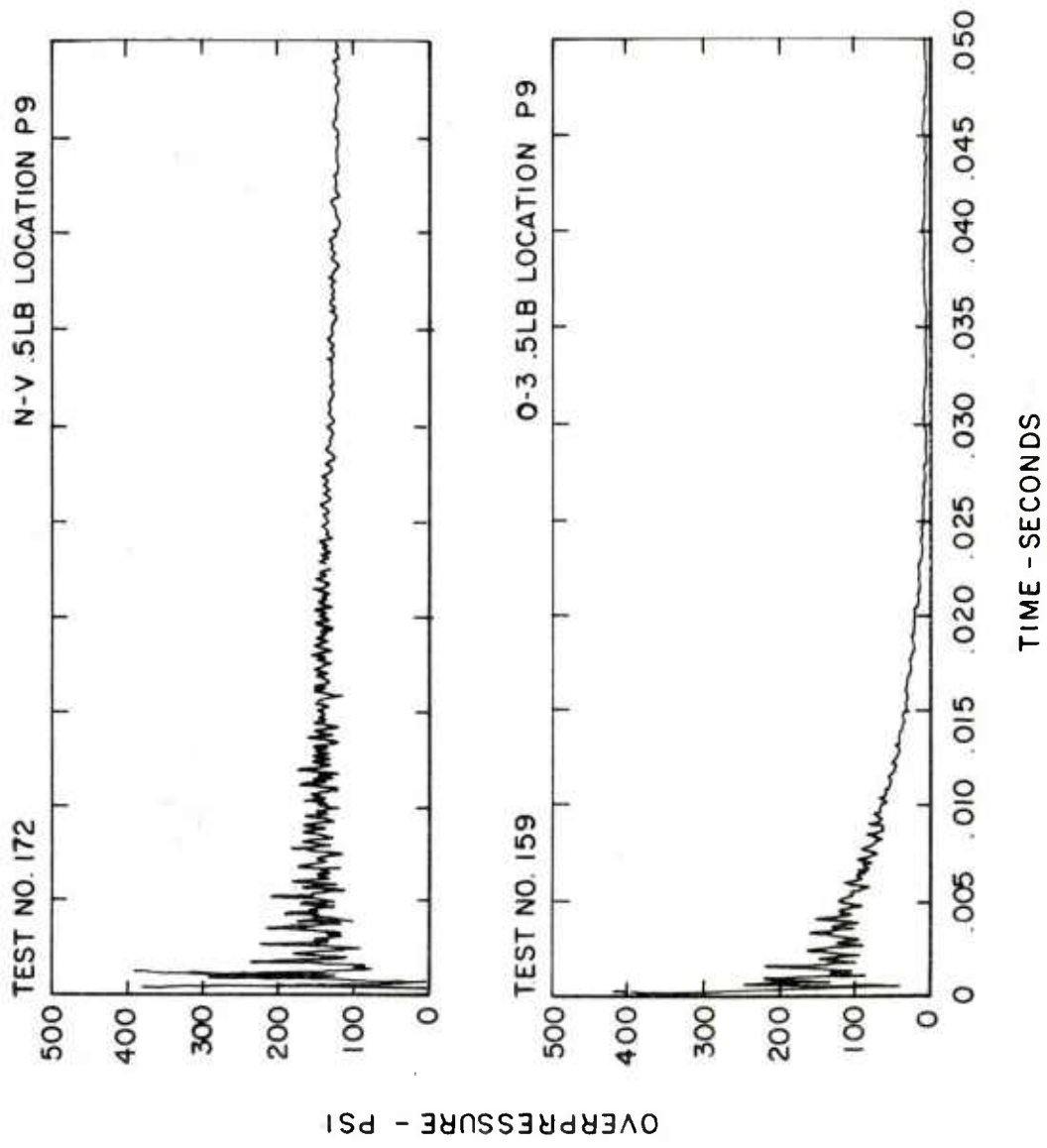


Figure 24. Comparison of Internal Pressure versus Time Recorded in Structure N-V and Structure O-3

a zero overpressure in approximately 0.7 second. Also shown in Figure 24 is the internal pressure recorded in structure 0-3. This comparison is presented to show the difference in the internal pressure loading on the wall of a vented and non-vented structure.

5. Internal Pressure in Structure T-5 and 0-4 from 1 Pound Charges.

Both one pound and one-half pound pentolite charges were detonated in each structure. Only a few representative records from the one pound charges will be presented for comparison and discussion because the trends are similar and conclusions would be the same as established for the one-half pound charges.

In Figure 23 a comparison was presented showing the similarity in the internal pressure and decay rate in structure T-5 and structure 0-4 when a 0.5 pound charge was detonated in the geometric center of each structure. A similar comparison is presented in Figure 25 where the pressures recorded for the detonation of 1.0 pound charges are presented for the same two structures. The two records in Figure 25 show very similar pressure fluctuations and decay rates.

6. Internal Pressure in Structure 0-3 from 0.5 and 1.0 Pound Charges.

A comparison of the internal pressure versus time recorded at P9 from the explosion of a 0.5 pound and 1.0 pound spherical charge is presented in Figure 26. The primary differences are the peak internal gas pressure, the magnitude of the internal reflections and the rate of decay of the overpressure.

E. Internal Pressure versus Time Predictions

There are several methods reported in the literature for predicting the peak internal gas pressure generated from detonations in closed and partially closed chambers^{1,5,7,10}. Reference 5 is believed to be the best source available for calculating the internal pressure versus time and therefore it has been set in operation at BRL on the BRLESC computer. Runs were made for the charge weights, volume and several vent areas related to the 1/16 size structures being tested.

1. Internal Pressure versus Time for Structures with Different Vent Areas. Computer runs were made using the Proctor code⁵ for the sub-scale structures with different vent areas and a 0.5 pound charge. The output was plotted as internal pressure versus time for the different vent areas and is plotted in Figure 27. This figure shows the effect of vent area on the rate of decay of internal pressure versus time. The rate of decay of the internal pressure within the different structures has been recorded but the effective vent area is the unknown variable, therefore in Figure 28, the computer output was plotted using time versus percent vent area for constant internal pressure. Here a measured record can be matched with the pressure versus time along a vertical scale and the effective percent vent area can be estimated or if the effective percent vent area is known a pressure versus time can be predicted.

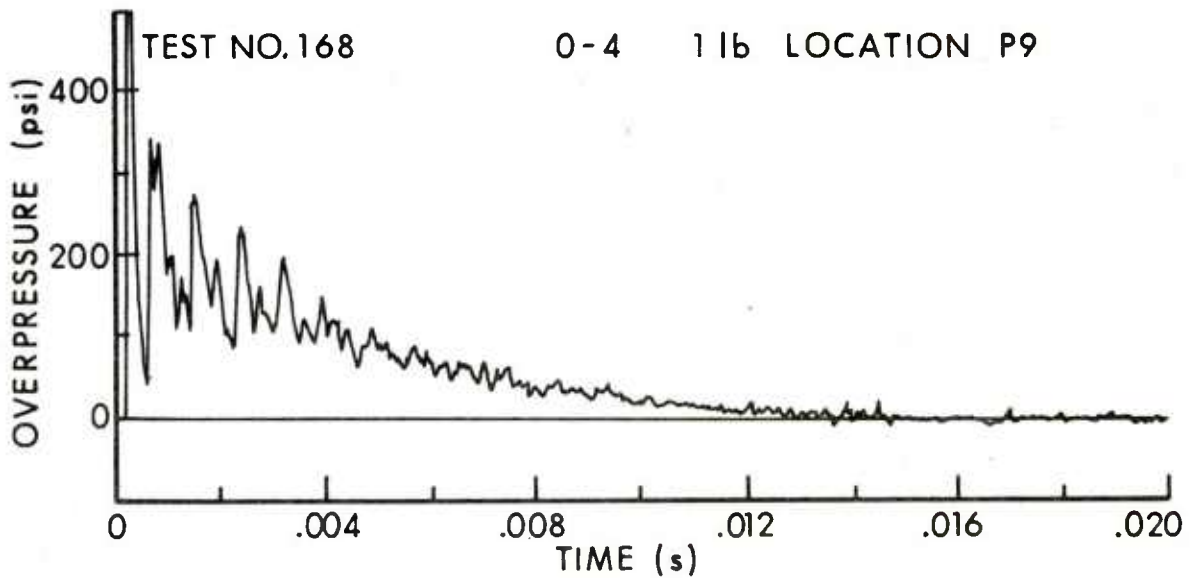
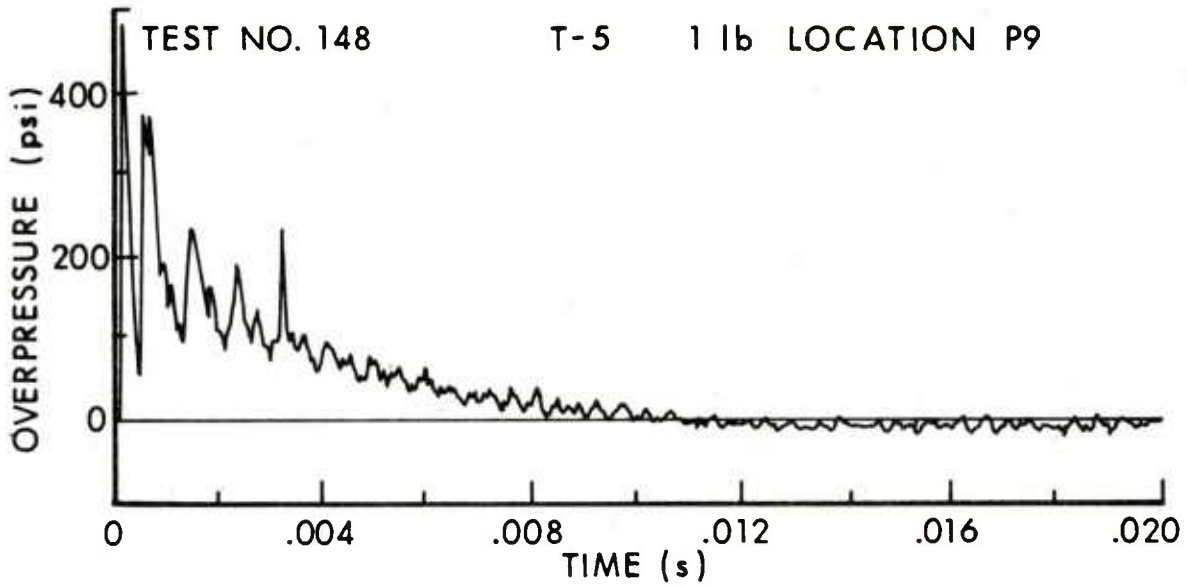


Figure 25. Comparison of Internal Pressure versus Time Recorded in Structure T-5 and Structure 0-4, 1.0 Pound Charge

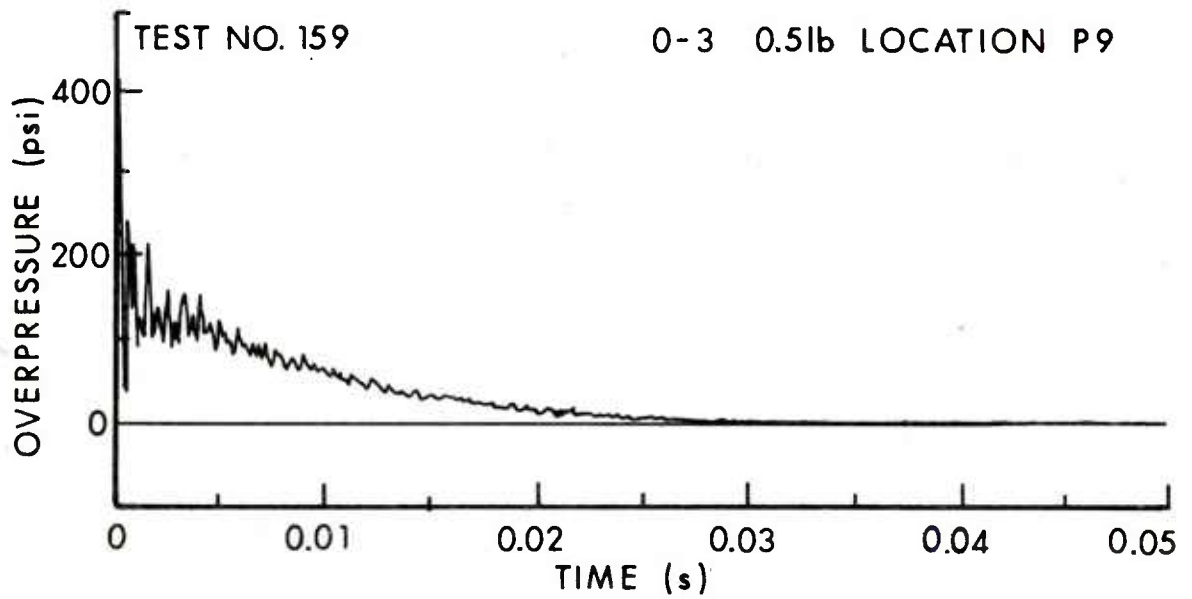
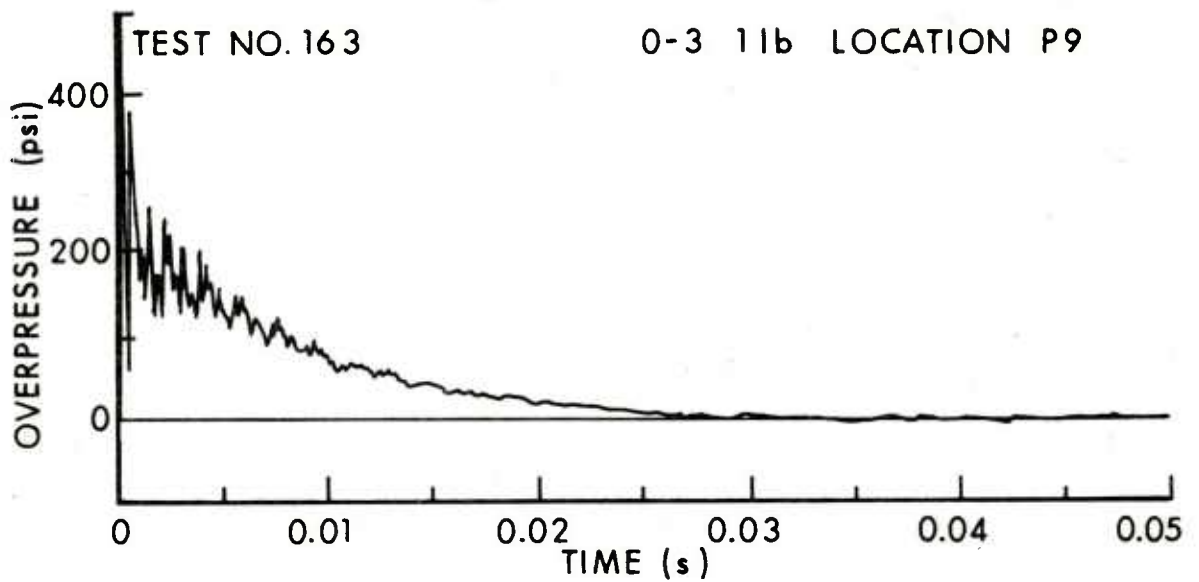


Figure 26. Comparison of Internal Pressure versus Time Recorded in Structure 0-3 from 0.5 and 1.0 Pound Charges

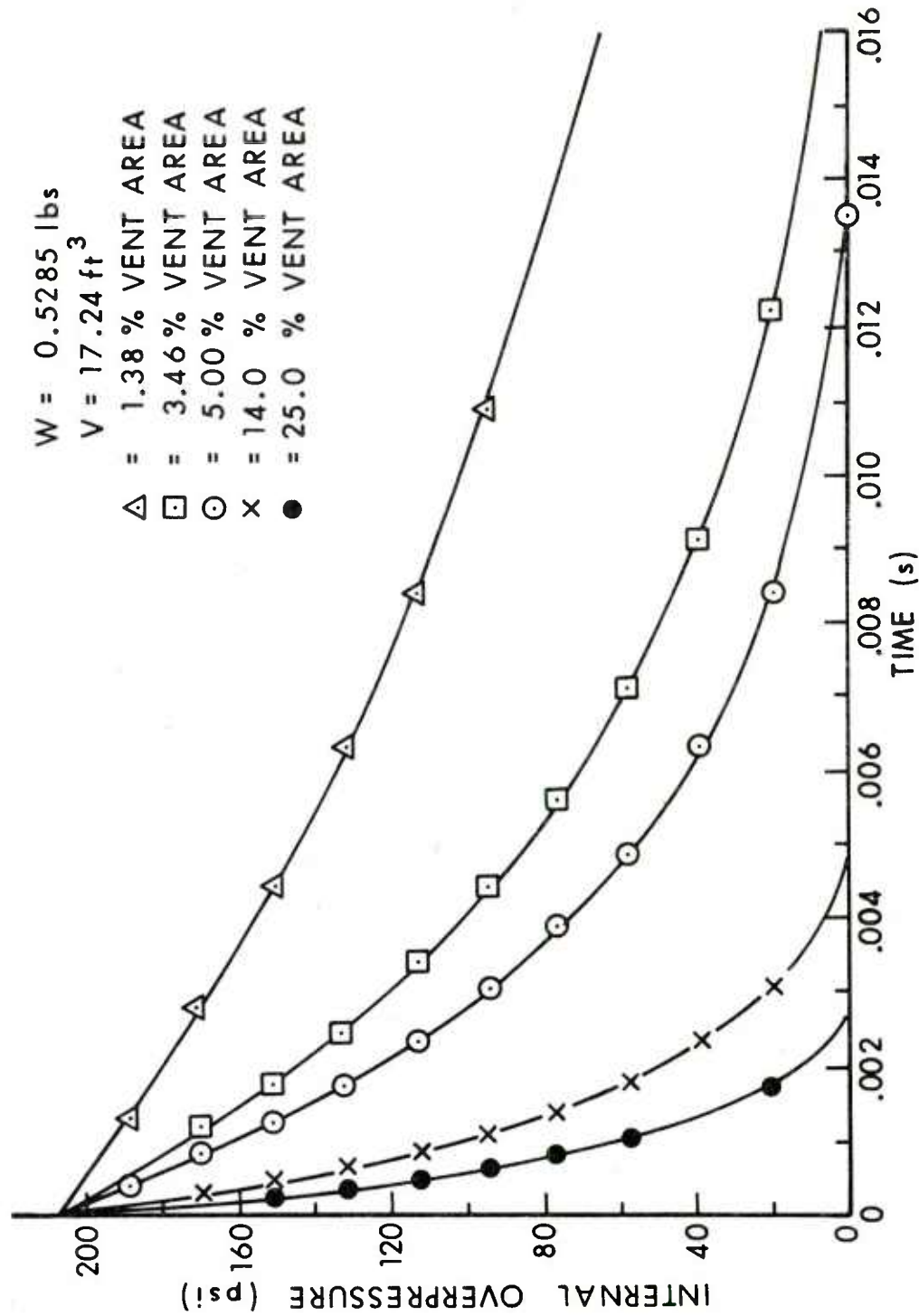


Figure 27. Computed Internal Pressure versus Time for Different Vent Areas

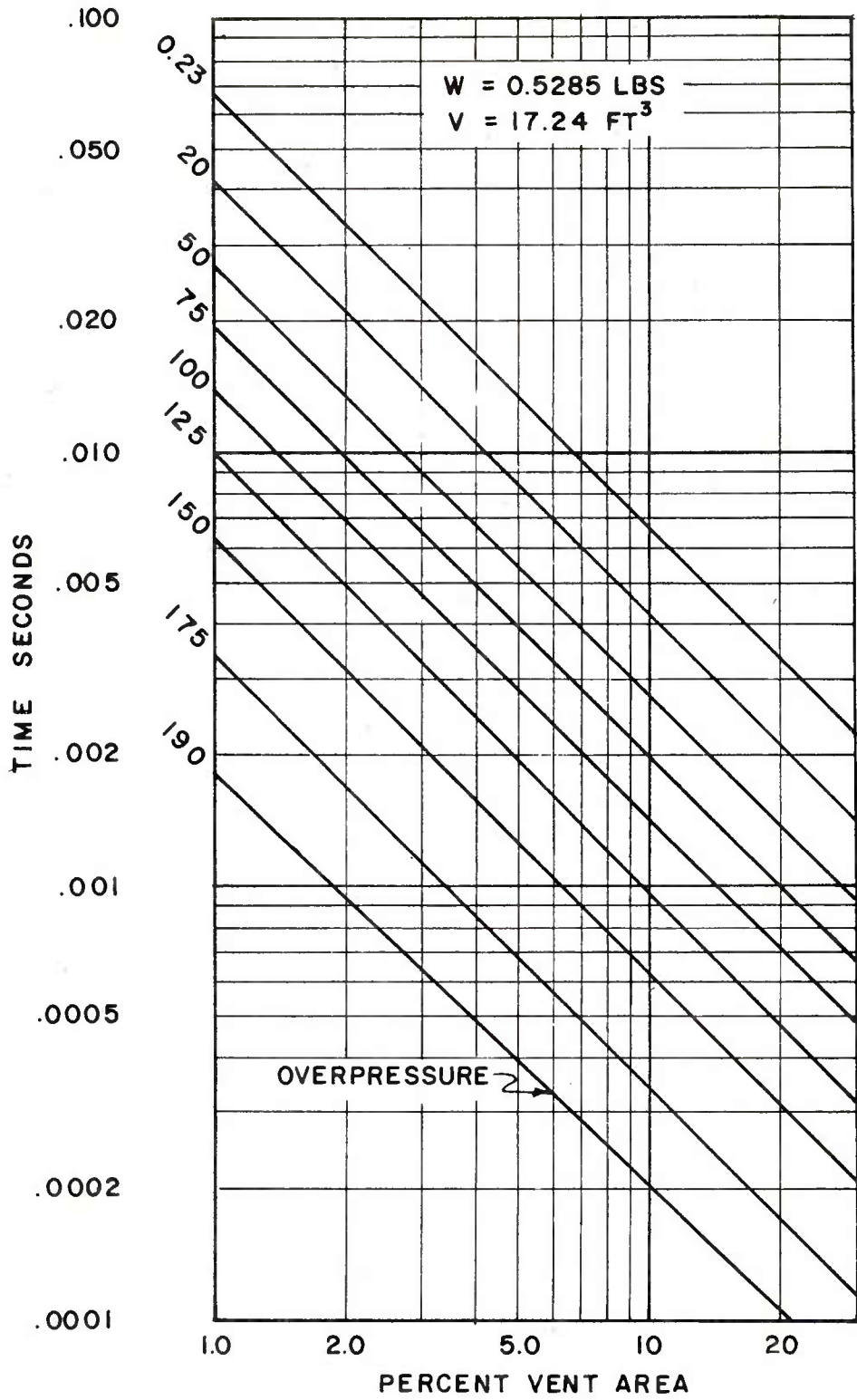


Figure 28. Computed Time versus Vent Area for Constant Internal Pressure, 0.5 Pound Charge

Computer runs were made for a one pound spherical charge in the same structure volume with similar vent areas. From the computer output several plots of time versus percent vent area for constant overpressure were developed. These curves are presented in Figure 29.

2. Comparison of Measured Records and Computer Output. The effective vent areas (A_v) established in Table IV were used for comparing the quasi-static pressure versus time predicted from Figures 28 and 29 with selected measured records.

A selected example showing the comparison of a measured record from structure T-1 and the predicted computer record for a vent area determined from Table IV is presented in Figure 30. The internal pressure versus time for a 9.3 percent vent area appears to give a good fit to the recorded data. The peak internal gas pressure from the computer program was 220 psi for the .5 pound charge weight, compared to 214 psi measured average.

The same method was used to determine a complete pressure versus time for a 4.7 percent effective vent area for structure T-5. The comparison is presented in Figure 31. Here it can be seen that a vent area of 4.7 percent shows a good fit to the measured records.

In Figure 23 it was shown that the internal pressure versus time recorded in structure T-5 and 0-4 was quite similar. This is shown again in Figure 32 where a 4.7 percent vent area calculation from the computer program appears to also be an adequate fit to the measured internal pressure versus time from structure 0-4.

For structure 0-3 the percent vent area predicted by BRL in Table I was one-half that of structure 0-4. The effective vent area based on duration (t_g) and listed in Table IV is 2.4 percent for structure 0-3 which is very nearly one-half the value determined for structure 0-4. In Figure 33 the internal pressure versus time (for a 2.4 percent vent area using Figures 28 and 29) is plotted with the records obtained in structure 0-3 for the two charge weights to show the correlation of the records and computer program

3. A Second Method for Determining the Internal Pressure Decay Rate. In Reference 10 a rather simple equation was developed whereby the internal pressure versus time can be calculated if the maximum value, the vent area and the volume of the structure are known. The equation is given as follows:

$$\text{Log } P = \text{Log } P_{\text{max}} - .315 \left(\frac{A_v}{V} \right) t_s \quad (7)$$

P = Pressure (atmospheres)

P_{Max} = maximum pressure (atmospheres)

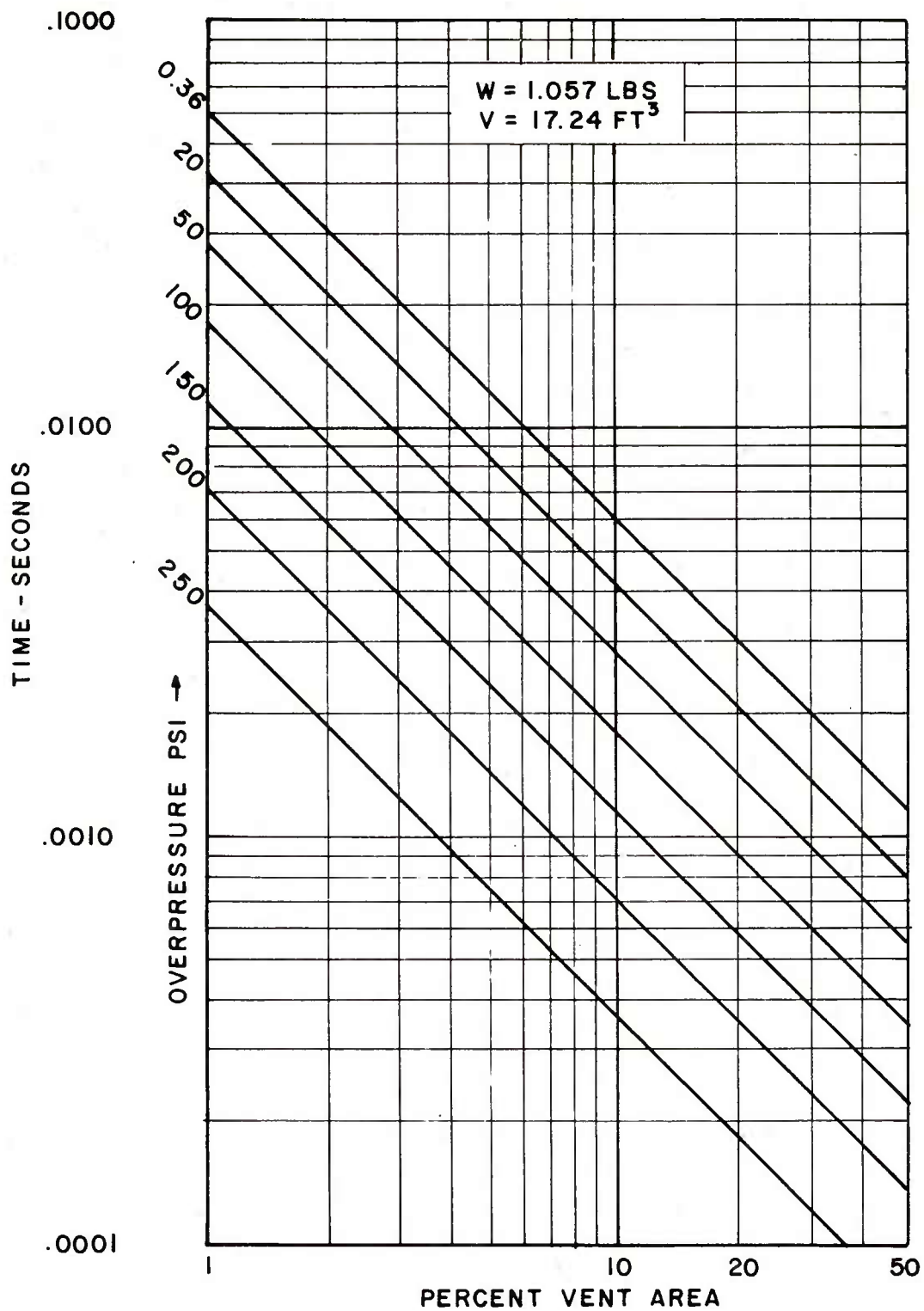


Figure 29. Computed Time versus Vent Area for Constant Pressure, 1.0 Pound Charge

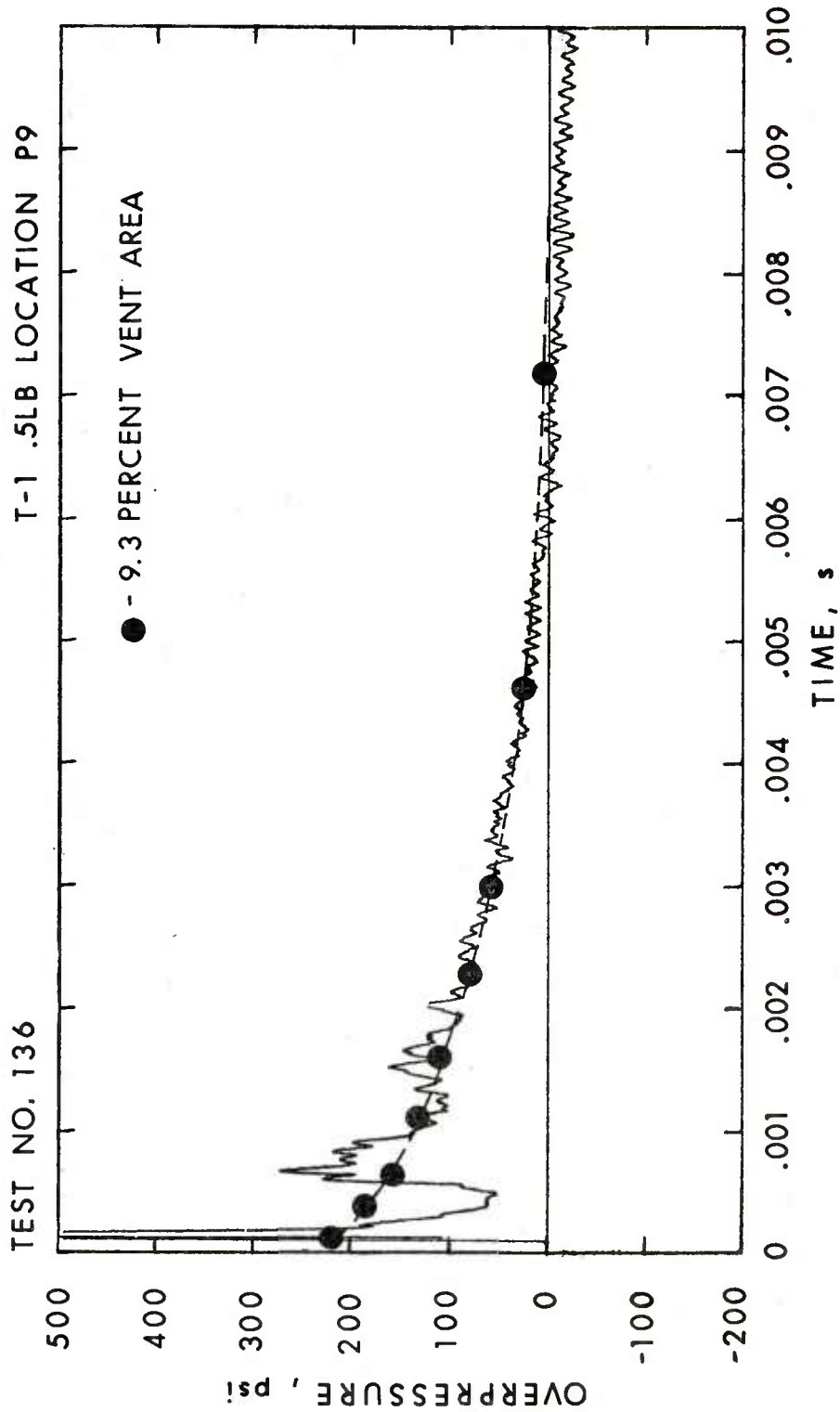


Figure 30. Comparison of Measured Data from T-1 and the Computer Output for a 9.3 Percent Vent Area

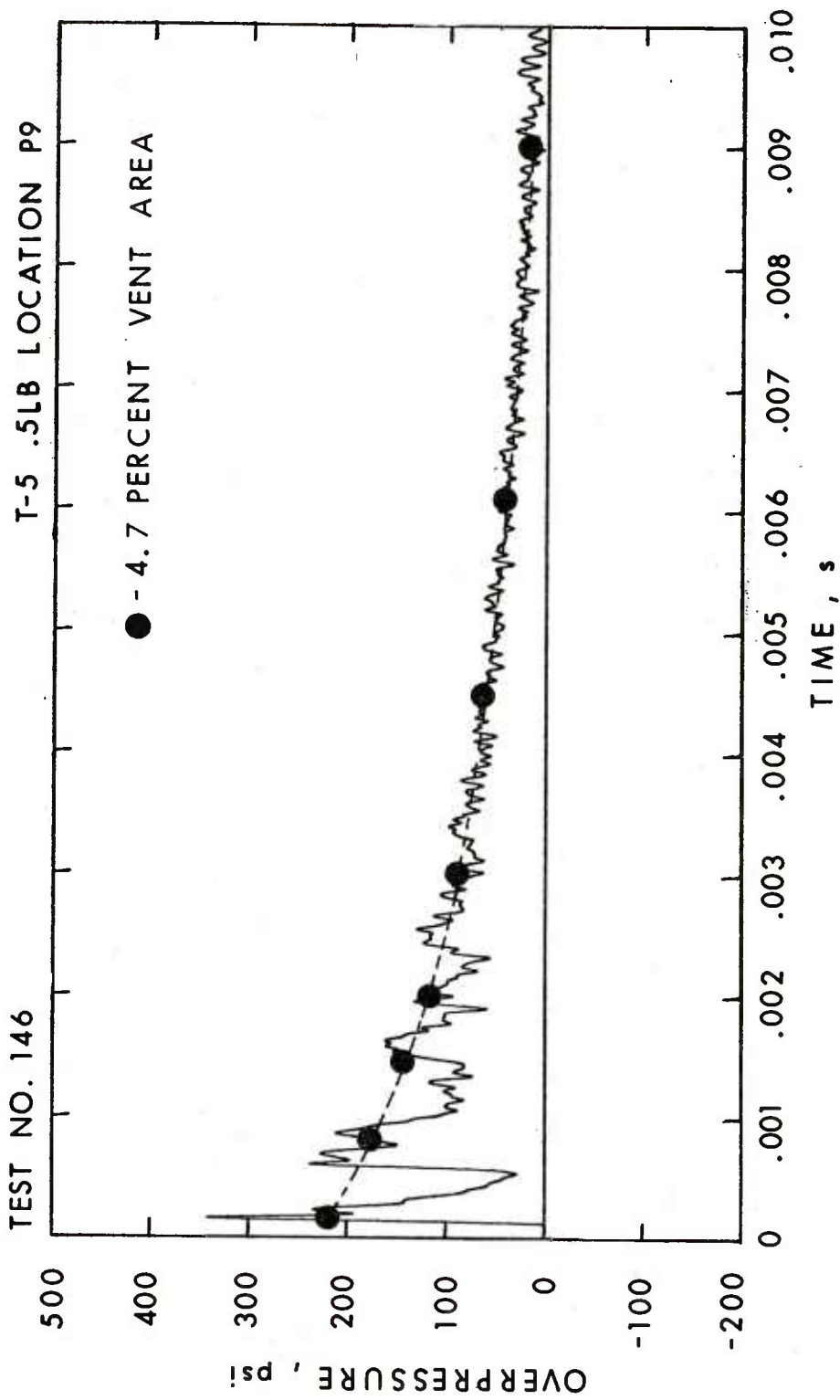


Figure 31. Comparison of Measured Data from T-5 and Computer Output for a 4.7 Percent Vent Area

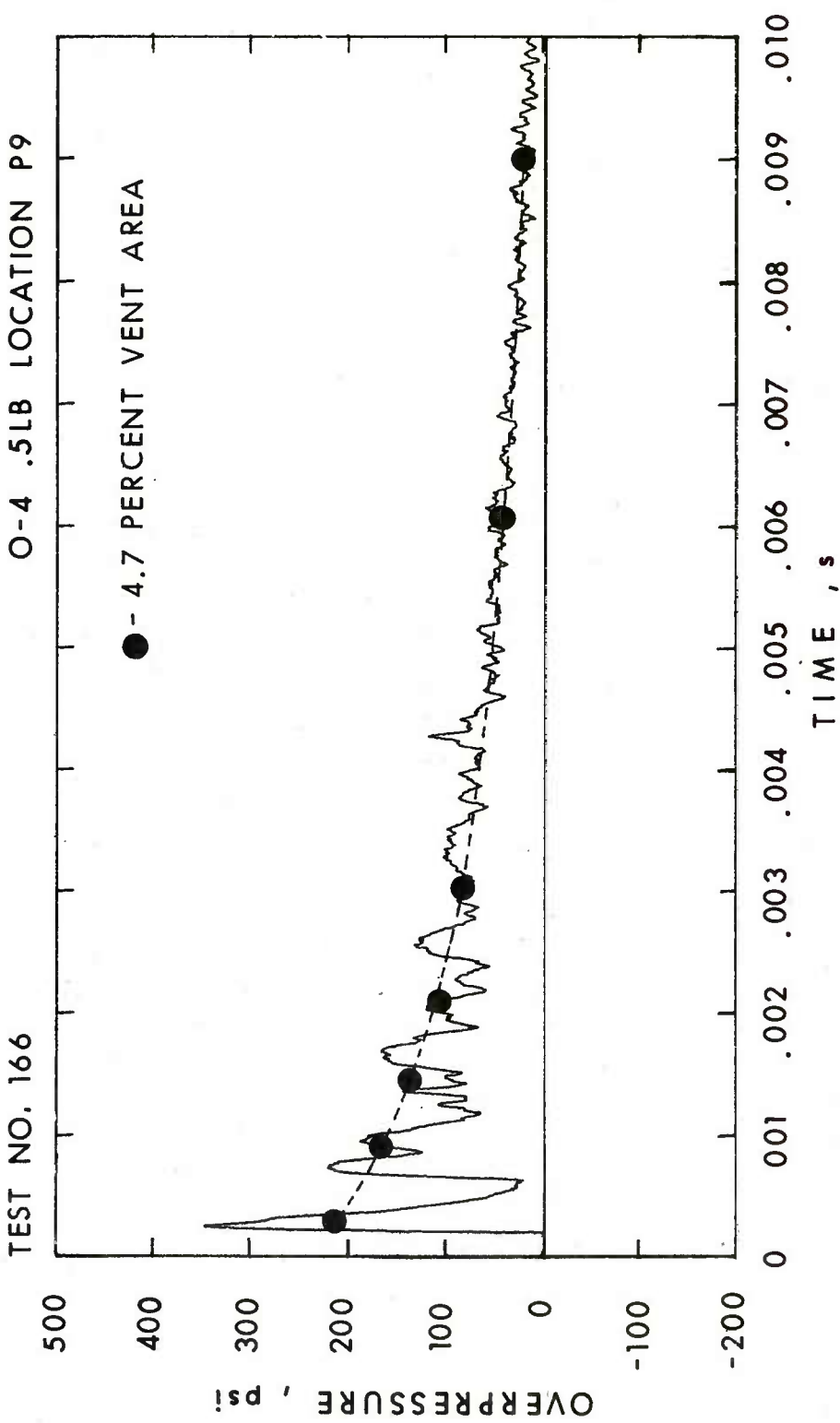


Figure 32. Comparison of Measured Data from Structure 0-4 and Computer Output for a 4.7 Percent Vent Area

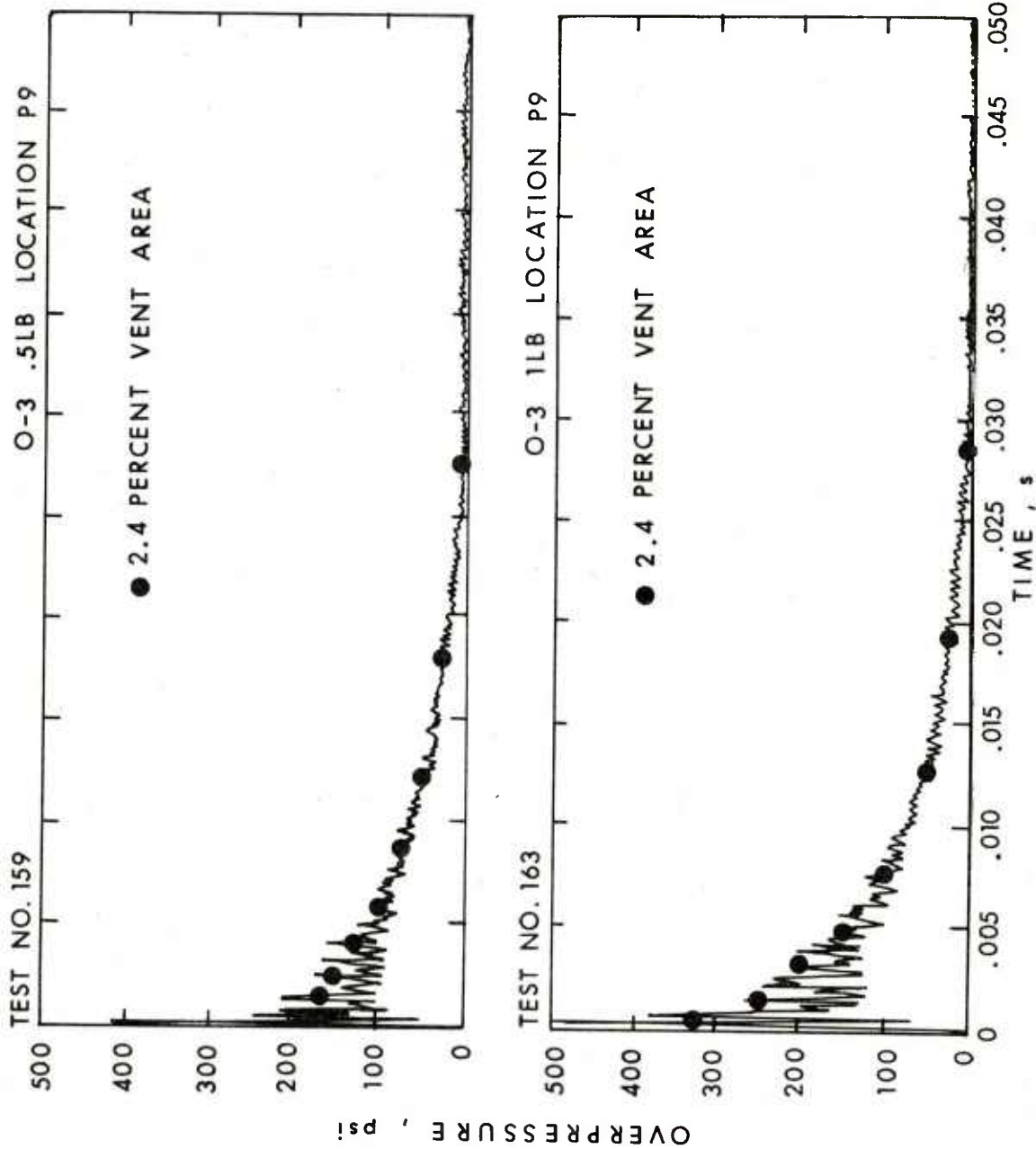


Figure 33. Comparison of Measured Data from Structure 0-3 and Computer Output for 2.4 Percent Vent Area for Two Charge Weights

A_V = Vent Area, square meters

V = Structure volume, cubic meters

t_s = time (milliseconds).

Calculations were made for a 4.7 percent vent area. A comparison of the internal pressure versus time obtained from the Proctor computer code and the Sewell-Kinney equation given above is presented in Figure 34, along with the measured values from structure 0-4. The comparison between the two methods and the record shows excellent agreement.

IV. CONCLUSION

The first conclusion to be drawn is that the stated objectives of the program have been achieved. Other specific conclusions reached from an analysis of the results are listed as follows:

1. There are two methods (Reference 5 and 10) that appear adequate for predicting the internal gas pressure versus time over the range of tests conducted in this program if the effective vent areas are known.

2. The method devised by SwRI and used by BRL to calculate the effective vent area based on blast attenuation outside the structure does not apply to effective vent areas determined from the decay of internal pressure and computer calculations.

3. The third conclusion is that there is a need for more basic data on the decay rate of internal pressure versus known vent areas. This should be done with the same experimental layout and a structure with single plate walls of known vent area.

TEST NO. 168

0-4 1 .LB LOCATION P9

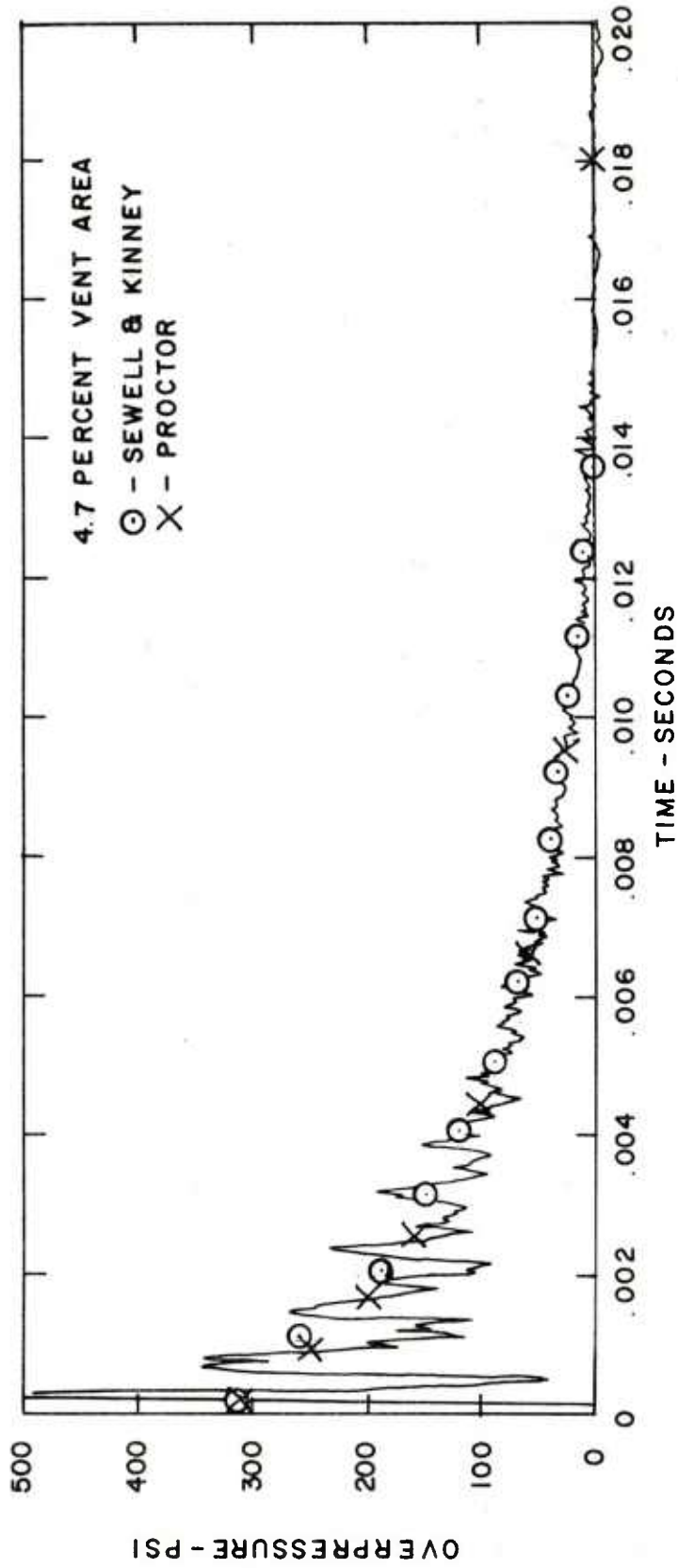


Figure 34. Comparison of Two Prediction Methods of Internal Pressure versus Time with Measured Data

LIST OF SYMBOLS

A_i	Vent area for each individual venting element of a wall, ft^2
P_{QE}	Quasi-static pressure - extrapolated to zero rise time, psi
P_{QA}	Quasi-static pressure - average at a time equal to $W^{2/3}$ msec for W/V of .01 to .06
A_v	Vented Area, ft^2
V	Volume, ft^3
W	Charge Weight, lbs.
t_g	Duration of quasi-static pressure, msec
I_g	Impulse of quasi-static pressure, psi-msec

REFERENCES

1. Baker, W.E., Westine, P.S., et al, "Analysis and Preliminary Design of a Suppressive Structure for a Melt Loading Operation," Tech. Report No. 1, Southwest Research Institute, San Antonio, Texas, March 4, 1974.
2. Kingery, C. and Pannill, B., "Parametric Analysis of the Regular Reflection of Air Blast," BRL Report 1249, June 1964. (AD #444997)
3. Minutes of the Fifteenth Explosives Safety Seminar, Giglio Tos, L., Linnenbrink, T., "Airblast Pressure Measurement Systems and Techniques," pp 1359 - 1402, September 1973.
4. Jack, W. H., "Measurements of Normally Reflected Shock Waves from Explosive Charges," BRL Memo Report No. 1499, July 1963. (AD #422886)
5. Proctor, J. and Lorenz, R. A., "Internal Blast Computer Program," NSWC/WOL TR 75-183 (To be published).
6. Schumacher, R., Kingery, C., and Ewing, W. Jr., "Airblast and Structural Response Testing of a 1/4 Scale Category I Suppressive Structure," BRL Memo Report.
7. Minutes of the Fourteenth Explosives Safety Seminar, Keenan, W. A. and Tancreto, J. E., "Effects of Venting and Frangibility on Blast Environment from Explosions in Cubicles," pp 125 - 161, Nov. 1973.
8. Minutes of the Sixteenth Explosives Safety Seminar, Keenan, W. A. and Tancreto, J. E., "Blast Environment from Fully and Partially Vented Explosives in Cubicles," pp 1527 - 1559, Sept. 1974.
9. 61-JTCG/ME-73-3 Joint Technical Coordinating Group for Munition Effectiveness, Proctor, J. F., "Internal Blast Damage Mechanism Computer Program," 10 April 1973.
10. Kinney, G. F. and Sewell, R. G. S., "Venting of Explosives," NWC Tech Memo 2448, July 1974.

DISTRIBUTION LIST

<u>No. of</u> <u>Copies</u>	<u>Organization</u>	<u>No. of</u> <u>Copies</u>	<u>Organization</u>
12	Commander Defense Documentation Center ATTN: DDC-TCA Cameron Station Alexandria, VA 22314	1	Director Defense Communications Agency ATTN: NMCSSC (Code 510) Washington, DC 20305
1	Director Defense Advanced Research Projects Agency 1400 Wilson Boulevard Arlington, VA 22209	2	Director Defense Intelligence Agency ATTN: DT-1C, Dr. J. Vorona DIR-4C3, R. Sauer Washington, DC 20301
1	Director of Defense Research & Engineering Department of Defense Washington, DC 20301	2	Director Defense Nuclear Agency ATTN: Mr. J. F. Moulton, SPAS Dr. E. Sevin, SPSS Washington, DC 20305
1	Director Weapons Systems Evaluation Gp. ATTN: CPT Donald E. McCoy Washington, DC 20305	4	Director Defense Nuclear Agency ATTN: SPTL Tech Lib (2 cys) APSI (ARCHIVES) LGLS, Mr. E. L. Eagles Washington, DC 20305
3	Director Institute for Defense Analyses ATTN: Dr. J. Menkes Dr. J. Bengston Tech Info Ofc 400 Army-Navy Drive Arlington, VA 22202	1	Commander Field Command Defense Nuclear Agency ATTN: Tech Lib, FCWS-SC Kirtland AFB, NM 87115
1	Office Secretary of Defense Director of Defense Rsch & Eng. ATTN: Mr. J. Persh, Staff Specialist, Materials and Structures Washington, DC 20301	1	Chief Las Vegas Liaison Office Field Command TD, DNA ATTN: Document Control P. O. Box 2702 Las Vegas, NV 89104
1	Assistant Secretary of Defense (MRA&L) ATTN: ID (Mr. H. Metcalf) Washington, DC 20301	1	DNA Information and Analysis Center TEMPO, General Electric Co. Center for Advanced Studies ATTN: DASIAC 816 State Street Santa Barbara, CA 93102
1	Assistant to the Secretary of Defense (Atomic Energy) ATTN: Document Control Washington, DC 20301		

DISTRIBUTION LIST

<u>No. of Copies</u>	<u>Organization</u>	<u>No. of Copies</u>	<u>Organization</u>
1	Defense Civil Preparedness Agency ATTN: David W. Benson Washington, DC 20301	1	Director US Army Air Mobility Research and Development Laboratory Ames Research Center Moffett Field, CA 94035
5	Chairman DOD Explosives Safety Board Room 856-C, Hoffman Bldg. I 2461 Eisenhower Avenue Alexandria, VA 22331	1	Commander US Army Electronics Research and Development Command ATTN: DELSD-L Tech Support Activity Fort Monmouth, NJ 07703
2	Chairman Joint Chiefs of Staff ATTN: J-3, Operations J-5, Plans & Policy (R&D Division) Washington, DC 20301	1	Commander US Army Communications Rsch and Development Command ATTN: DRDCO-SGS Fort Monmouth, NJ 07703
2	Director Joint Strategic Target Planning Staff ATTN: JLTW TPTP Offutt AFB, Omaha, NB 68113	4	Commander US Army Missile Research and Development Command ATTN: DRDMI-R DRDMI-RSS, Mr. B. Cobb DRDMI-RX, Mr. W. Thomas DRDMI-RR, Mr. L. Lively Redstone Arsenal, AL 35809
1	Commander US Army Materiel Development and Readiness Command ATTN: DRCDMD-ST 5001 Eisenhower Avenue Alexandria, VA 22333	1	Commander US Army Missile Materiel Readiness Command ATTN: DRSMI-AOM Redstone Arsenal, AL 35809
1	Commander US Army Materiel Development and Readiness Command ATTN: Mr. W.G. Queen, DRCSF 5001 Eisenhower Avenue Alexandria, VA 22333	2	Commander US Army Tank Automotive Research & Development Cmd ATTN: DRDTA DRDTA-UL Warren, MI 48090
1	Commander US Army Aviation Research and Development Command ATTN: DRSAV-E 12th and Spruce Streets St. Louis, MO 63166	1	Commander US Army Mobility Equipment Research & Development Cmd ATTN: DRDFB-ND Fort Belvoir, VA 22060

DISTRIBUTION LIST

<u>No. of Copies</u>	<u>Organization</u>	<u>No. of Copies</u>	<u>Organization</u>
3	Commander US Army Armament Research and Development Command ATTN: DRDAR-TSS (2 cys) DRDAR-LC Dover, NJ 07801	1	Commander Iowa Army Ammunition Plant Burlington, IA 52502
2	Commander US Army Armament Materiel Readiness Command ATTN: DRSAR-LEP-L, Tech Lib DRSAR-SA Rock Island, IL 61299	1	Commander Joliet Army Ammunition Plant Joliet, IL 60436
3	Commander US Army Armament Materiel Readiness Command ATTN: Joint Army-Navy-Air Force Conventional Ammunition Prof Coord Gp/ E. Jordan Rock Island, IL 61299	1	Commander Kansas Army Ammunition Plant Parsons, KS 67357
1	Commander US Army Rock Island Arsenal Rock Island, IL 61299	1	Commander Lone Star Army Ammunition Plant Texarkana, TX 75502
1	Commander Dugway Proving Ground ATTN: STEDP-TO-H, Mr. Miller Dugway, UT 84022	1	Commander Longhorn Army Ammunition Plant Marshall, TX 75671
1	Commander US Army Watervliet Arsenal Watervliet, NY 12189	1	Commander Louisiana Army Ammunition Plant Shreveport, LA 71102
1	Commander Pine Bluff Arsenal Pine Bluff, AR 71601	1	Commander Milan Army Ammunition Plant Milan, TN 38358
1	Commander Cornhusker Army Ammunition Plant Grand Island, NE 68801	1	Commander Radford Army Ammunition Plant Radford, VA 24141
1	Commander Indiana Army Ammunition Plant Charlestown, IN 47111	1	Commander Ravenna Army Ammunition Plant Ravenna, OH 44266
		1	Commander US Army Harry Diamond Labs ATTN: DELHD-TI 2800 Powder Mill Road Adelphi, MD 20783
		1	Commander US Army Materials and Mechanics Research Center ATTN: DRXMR-ATL Watertown, MA 02172

DISTRIBUTION LIST

<u>No. of Copies</u>	<u>Organization</u>	<u>No. of Copies</u>	<u>Organization</u>
1	Commander US Army Natick Research and Development Command ATTN: DRXRE, Dr. D. Sieling Natick, MA 01762	1	Office of the Inspector General Department of the Army ATTN: DAIG-SD Washington, DC 20310
1	Commander US Army Foreign Science and Technology Center ATTN: Rsch & Data Branch Federal Office Building 220 - 7th Street, NE Charlottesville, VA 22901	1	HQDA (DAMO-ODC, COL G. G. Watson) Washington, DC 20310
1	Director DARCOM Field Safety Activity ATTN: DRXOS-ES Charlestown, IN 47111	1	HQDA (DAEN-MCE-D, Mr. R. Wright) Washington, DC 20314
1	Director DARCOM, ITC ATTN: Dr. Chiang Red River Depot Texarkana, TX 75501	1	HQDA (DAEN-MCC-D, Mr. L. Foley) Washington, DC 20314
1	Commander US Army TRADOC Systems Analysis Activity ATTN: ATAA-SL, Tech Lib White Sands Missile Range NM 88002	1	HQDA (DAEN-RDL) Washington, DC 20314
1	Director US Army Engineer School Fort Belvoir, VA 22060	1	Division Engineer US Army Engineer Division Fort Belvoir, VA 22060
1	Commander US Army Nuclear Agency 7500 Backlick Rd, Bldg 2073 Springfield, VA 22150	1	US Army Eng Div ATTN: Mr. Char P. O. Box 1600 Huntsville, AL 35809
1	HQDA (DAMA-CSM-CA) Washington, DC 20310	1	Commander US Army Construction Engineering Research Laboratory P. O. Box 4005 Champaign, IL 61820
2	HQDA (DAMA-AR; NCL Div) Washington, DC 20310	1	Director US Army Engineer Waterways Experiment Station ATTN: WESNS, Mr. J. M. Watt P. O. Box 631 Vicksburg, MS 39180
		1	Commander US Army Research Office P. O. Box 12211 Research Triangle Park NC 27709

DISTRIBUTION LIST

<u>No. of Copies</u>	<u>Organization</u>	<u>No. of Copies</u>	<u>Organization</u>
1	Director US Army Advanced BMD Technology Center ATTN: M. Whitfield Huntsville, AL 35807	1	Commander Naval Ordnance Systems Command ATTN: Code ORD-43B Mr. Fernandes Washington, DC 20360
1	Commander US Army Ballistic Missile Defense Systems Command ATTN: J. Veeneman P. O. Box 1500, West Station Huntsville, AL 35807	2	Commander Naval Sea Systems Command ATTN: SEA-04H, Mr. C.P. Jones SEA-0333 Washington, DC 20360
1	Commander US Army Europe ATTN: AEAGB (S&E) APO New York 09403	2	Commander David W. Taylor Naval Ship Research & Development Ctr ATTN: Mr. A. Wilner, Code 1747 Dr. W.W. Murray, Code 17 Bethesda, MD 20084
4	Chief of Naval Operations ATTN: OP-41B, CPT S.N.Howard OP-411, J. W. Connelly OP-754 OP-985FZ Department of the Navy Washington, DC 20350	3	Commander Naval Surface Weapons Center ATTN: CT-23 Mr. J. C. Talley Dr. W. Soper Dahlgren, VA 22448
1	Assistant Secretary of the Navy (Research & Development) Navy Department Washington, DC 20350	3	Commander Naval Surface Weapons Center ATTN: Dr. Leon Schindel Dr. Victor Dawson Dr. P. Huang Silver Spring, MD 20910
1	Commander Bureau of Naval Weapons ATTN: Code F121, H. Roylance Department of the Navy Washington, DC 20360	2	Commander Naval Weapons Center ATTN: Code 0632 China Lake, CA 93555
1	Commander Naval Air Systems Command ATTN: AIR-532 Washington, DC 20361	1	Commander Naval Weapons Support Center ATTN: NAPEC Crane, IN 47522

DISTRIBUTION LIST

<u>No. of Copies</u>	<u>Organization</u>	<u>No. of Copies</u>	<u>Organization</u>
2	Commander Naval Explosive Ord Disposal Facility ATTN: Code 501, L. Wolfson Code D Indian Head, MD 20640	1	AFSC (DSCPSL) Andrews AFB Washington, DC 20331
1	Commander Naval Ship Research and Development Ctr Facility ATTN: Mr. Lowell T. Butt Underwater Explosions Research Division Portsmouth, VA 23709	1	HQ AFSC (IGFG) Andrews AFB Washington, DC 20334
1	Commander Naval Weapons Evaluation Facility ATTN: Document Control Kirtland AFB Albuquerque, NM 87117	1	AFRPL (M. Raleigh) Edwards AFB, CA 93523
1	Commander Naval Civil Engineering Lab ATTN: Code L51 Port Hueneme, CA 93041	1	ADTC (ADBPS-12) Eglin AFB, FL 32542
1	Commander Naval Research Laboratory ATTN: Code 2027, Tech Lib Washington, DC 20375	2	AFATL (ATRD, R. Brandt) Eglin AFB, FL 32542
2	Superintendent Naval Postgraduate School ATTN: Tech Reports Sec Code 57, Prof. R. Ball Monterey, CA 93940	1	AFATL (DLYV, R. L. McGuire) Eglin AFB, FL 32542
1	HQ USAF (AFNIE-CA) Washington, DC 20330	1	USAFTAWC (OA) Eglin AFB, FL 32542
4	HQ USAF (AFRIDQ; AFRDOSM; AFRDPM; AFRD) Washington, DC 20330	1	Ogden ALC/MMWRE ATTN: Mr. Ted E. Comins Hill AFB, UT 84406
		3	AFWL (WLA; WLD; WLRP, LTC H. C. McClammy) Kirtland AFB, NM 87117
		5	AFWL (DEO, Mr. F.H. Peterson; SYT, MAJ W. A. Whitaker; SRR; WSUL; SR) Kirtland AFB, NM 87117
		1	Director of Aerospace Safety USAF/IGD/AFISC (SEV) COL G. J. Corak Norton AFB, CA 92409
		1	AFCEC-DE (LTC Walkup) Tyndall AFB Panama City, FL 32401

DISTRIBUTION LIST

<u>No. of Copies</u>	<u>Organization</u>	<u>No. of Copies</u>	<u>Organization</u>
1	AFFDL (FBE, Mr. R.M. Bader) Wright-Patterson AFB, OH 45433	1	Institute of Makers of Explosives ATTN: Mr. Harry Hampton Graybar Building, Rm 2449 420 Lexington Avenue New York, NY 10017
2	AFLC (MMWM/CPT D. Rideout; IGYE/K. Shopker) Wright-Patterson AFB, OH 45433	2	Battelle Columbus Laboratories ATTN: Dr. L. E. Hulbert Mr. J. E. Backofen, Jr. 505 King Avenue Columbus, OH 43201
4	AFML (MAMD, Dr. T. Nicholas; MAS; MANC, Mr. D. Schmidt; MAX, Dr. A.M. Lovelace) Wright-Patterson AFB, OH 45433	1	Director Lawrence Livermore Laboratory Technical Information Division P. O. Box 808 Livermore, CA 94550
1	FTD (ETD) Wright-Patterson AFB, OH 45433	1	Director Los Alamos Scientific Laboratory ATTN: Dr. J. Taylor P. O. Box 1663 Los Alamos, NM 87544
1	Headquarters Energy Research and Development Administration Dept of Military Applications Washington, DC 20545	2	Sandia Laboratories ATTN: Info Distr Division Dr. W. A. von Rieseemann Albuquerque, NM 87115
1	Director Division of Operational Safety Energy Research & Development Administration ATTN: Carlo Ferrara, Jr. Washington, DC 20545	2	Director Lewis Directorate US Army Air Mobility Research and Development Laboratory Lewis Research Center ATTN: Mail Stop 77-5 21000 Brookpark Road Cleveland, OH 44135
1	Albuquerque Operations Office Energy Research and Development Administration ATTN: ODI P. O. Box 5400 Albuquerque, NM 87115	1	Director National Aeronautics and Space Administration Marshall Space Flight Center Huntsville, AL 35812
1	Research Director - Pittsburgh Mining and Safety Research Center Bureau of Mines, Department of the Interior ATTN: Dr. Robert W. Van Dolah 4800 Forbes Avenue Pittsburgh, PA 15213		

DISTRIBUTION LIST

<u>No. of Copies</u>	<u>Organization</u>	<u>No. of Copies</u>	<u>Organization</u>
2	Director National Aeronautics and Space Administration Aerospace Safety Research and Data Institute ATTN: Mr. S. Weiss Mail Stop 6-2 Mr. R. Kemp Mail Stop 6-2 Lewis Research Center Cleveland, OH 44135	1	Black & Veatch Consulting Engineers ATTN: Mr. H. L. Callahan 1500 Meadow Lake Parkway Kansas City, MO 64114
		2	The Boeing Company Aerospace Group ATTN: Dr. Peter Grafton Dr. D. Strome Mail Stop 8C-68 Seattle, WA 98124
1	Director National Aeronautics and Space Administration Scientific and Technical Information Facility P. O. Box 8757 Baltimore/Washington International Airport, MD 21240	1	General American Research Div. General American Trans. Corp. ATTN: Dr. J. C. Shang 7449 N. Natchez Avenue Niles, IL 60648
1	National Academy of Sciences ATTN: Mr. D. G. Groves 2101 Constitution Avenue, NW Washington, DC 20418	1	Hercules, Inc. ATTN: Billings Brown Box 93 Magna, UT 84044
1	Aeronautical Research Assoc. of Princeton, Inc. ATTN: Dr. C. Donaldson 50 Washington Road Princeton, NJ 08540	1	J. G. Engineering Research Associates 3831 Menlo Drive Baltimore, MD 21215
1	Aerospace Corporation P. O. Box 95085 Los Angeles, CA 90045	2	Kaman-AviDyne ATTN: Dr. N. P. Hobbs Mr. S. Criscione Northwest Industrial Park 83 Second Avenue Burlington, MA 01803
1	Agbabian Associates ATTN: Dr. D. P. Reddy 250 N. Nash Street El Segundo, CA 90245	3	Kaman Sciences Corporation ATTN: Dr. F. H. Shelton Dr. D. Sachs Dr. R. Keefe 1500 Garden of the Gods Road Colorado Springs, CO 80907
2	AVCO Corporation Structures and Mechanics Dept. ATTN: Dr. William Broding Mr. J. Gilmore Wilmington, MA 01887		

DISTRIBUTION LIST

<u>No. of Copies</u>	<u>Organization</u>	<u>No. of Copies</u>	<u>Organization</u>
1	Knolls Atomic Power Laboratory ATTN: Dr. R. A. Powell Schenectady, NY 12309	1	Brown University Division of Engineering ATTN: Prof. R. Clifton Providence, RI 02912
2	Martin Marietta Laboratories ATTN: Dr. P. F. Jordan Mr. R. Goldman 1450 S. Rolling Road Baltimore, MD 21227	1	Georgia Institute of Tech ATTN: Dr. S. Atluri 225 North Avenue, NW Atlanta, GA 30332
1	Mason & Hangar-Silas Mason Company, Inc. Pantex Plant - ERDA ATTN: Director of Development P. O. Box 647 Amarillo, TX 79177	1	Lovelace Foundation ATTN: Dr. E. R. Fletcher P. O. Box 5890 Albuquerque, NM 87115
1	McDonnell Douglas Astronautics Western Division ATTN: Dr. Lea Cohen 5301 Bolsa Avenue Huntington Beach, CA 92647	1	Massachusetts Institute of Technology Aeroelastic and Structures Research Laboratory ATTN: Dr. E. A. Witmer Cambridge, MA 02139
1	Monsanto Research Corporation Mound Laboratory ATTN: Frank Neff Miamisburg, OH 45342	1	Ohio State University Dept of Engineering Mechanics ATTN: Prof. K. K. Stevens Columbus, OH 43210
1	Physics International 2700 Merced Street San Leandro, CA 94577	3	Southwest Research Institute ATTN: Dr. H. N. Abramson Dr. W. E. Baker Dr. U. S. Lindholm 8500 Culebra Road San Antonio, TX 78228
1	R&D Associates ATTN: Mr. John Lewis P. O. Box 9695 Marina del Rey, CA 90291	1	Stanford Research Institute ATTN: Dr. W. Reuland 306 Wynn Drive, NW Huntsville, AL 35805
1	Science Applications, Inc. 8th Floor 2361 Jefferson Davis Highway Arlington, VA 22202	1	Texas A & M University Dept of Aerospace Engineering ATTN: Dr. James A. Stricklin College Station, TX 77843

DISTRIBUTION LIST

<u>No. of Copies</u>	<u>Organization</u>
1	University of Alabama ATTN: Dr. T. L. Cost P. O. Box 2908 University, AL 35486
1	University of Delaware Department of Mechanical and Aerospace Engineering ATTN: Prof. J. R. Vinson Newark, DE 19711

Aberdeen Proving Ground

Dir, USAMSAA
ATTN: Dr. J. Sperrazza
Mr. R. Norman, GWD
Mr. N. Haggis, TDRAMD
Cdr/Dir, USA CSL, EA
ATTN: DRDAR-CLJ-L
Office of the Program Manager
for Demilitarization and
Installation Restoration
ATTN: DRXDC-T
Cdr, USATECOM
ATTN: DRSTE-SG-H